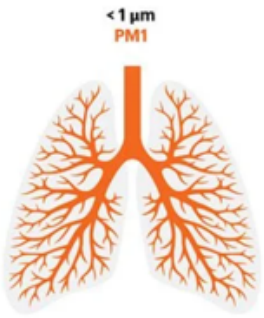

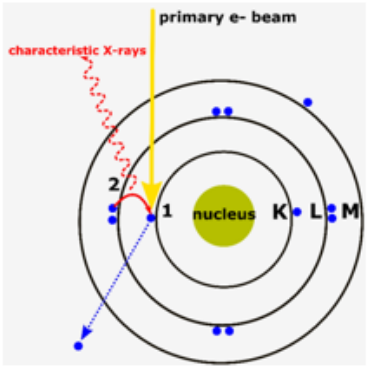

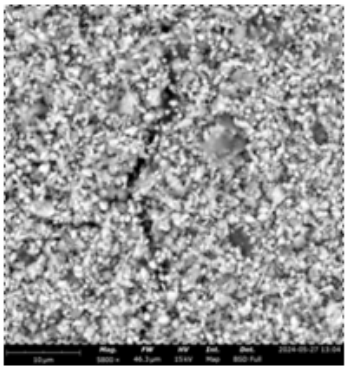

Assessment of brake wear emissions from a brake rig

Master's thesis in Mobility Engineering

NANDU SURESH

DEPARTMENT OF MECHANICS AND MARITIME SCIENCES

CHALMERS UNIVERSITY OF TECHNOLOGY
Gothenburg, Sweden 2024
www.chalmers.se

Master's Thesis in Mobility Engineering

Assessment of brake wear emissions from a brake rig

NANDU SURESH

CHALMERS
UNIVERSITY OF TECHNOLOGY

Department of Mechanics and Maritime Sciences
Division of Energy Conversion and Propulsion Systems
Chalmers University of Technology
Gothenburg, Sweden 2024

Assessment of brake wear emissions from a brake rig
NANDU SURESH

Supervisor: Jonas Sjöblom
Examiner: Jonas Sjöblom

Master's Thesis 2024
Department of Mechanics and Maritime Sciences
Chalmers University of Technology
SE-412 96 Gothenburg
Sweden
Telephone +46 31 772 1000

Cover: (Clockwise direction from top-left)- Brake system used for this project, Ultra-fine particles deep inside lungs (Source: SAFERA), Atom and k-shell of an element during SEM-EDX (Source: Thermo Fischer Scientific), Brake particles under an electron microscope at 5800x magnification.

Typeset in LaTeX
Gothenburg, Sweden 2024

Assessment of brake wear emissions from a brake rig
NANDU SURESH
Department of Mechanics and Maritime Sciences
Division of Energy Conversion and Propulsion Systems
Chalmers University of Technology

Abstract

As the number of vehicles on the road continues to rise, and solutions for exhaust emissions have been developed, non-exhaust emissions are becoming increasingly prominent, particularly brake wear emissions. Non-exhaust emissions could be extremely harmful to humans and can cause premature deaths. Hence it is necessary to identify the problematic particles among the brake particles to mitigate the harmful effect of brake wear emissions on health. This project aims to find the properties and composition of brake particles generated from a brake system comprising a brake disc and a pair of brake pads of a light-duty vehicle.

With multiple standardised driving cycles available, rig-based testing can be done with proper infrastructure, and brake particles can be sampled and analysed properly. The new upcoming Euro 7 legislation limits the PM10 emissions from the brakes of light-duty vehicles to 3 mg/km. Brake particles were generated using a custom drive cycle suitable for the operation of the brake rig, followed by the sampling and assessment of the particles using Dekati ELPI+ and further analysis was done using SEM-EDX to get microscopic pictures of brake dust as well as its chemical composition. For the test cycle and operating conditions, most of the particles formed were in the region of PM10. Particle size distribution (PSD) curves are plotted for a better understanding of different conditions like the re-suspension of brake particles. The effects of temperature, brake pressure and speed on the formation of brake particles are analysed in the form of PSD curves. Metals like Fe and Ca were found to be the dominant materials among the larger particles and elements like C, O, Si etc made up most of the smaller particles. Principal component analysis, together with SEM-EDX results validates that.

Keywords: Euro 7, Particulate Matter(PM), PM10, PM2.5, SEM, EDX, Brake wear, PSD, PCA, Respiratory health

Preface

This report presents the outcome of my master's thesis project carried out at the Department of Mechanics and Maritime Sciences at Chalmers University of Technology during the spring of 2024.

Acknowledgements

I express my sincere gratitude to my supervisor and examiner Dr. Jonas Sjöblom, who guided me throughout the thesis project with utmost care and led me towards the betterment of both my project and skills by providing constant feedback and giving me the urge to learn more each day.

I extend my sincere thanks to the senior research engineer at ECaPS, Robert Buadu, who helped me throughout the project with the experimentation part and taught me new things every day, and the other research engineers at ECaPS, especially Anders Mattsson who also helped me with the project, offering constant support and Patrik Wåhlin for his continuous support, advice and guidance.

Nandu Suresh, Gothenburg, September 2024

List of Acronyms

Below is the list of acronyms that have been used throughout this thesis listed in alphabetical order:

BWP	Brake Wear Particles
EDX	Energy-Dispersive X-ray Spectroscopy
ELPI	Electrical Low Pressure Impactor
EU	European Union
FTP	Federal Test Procedure
HEPA	High Efficiency Particulate Air [filter]
LDSA	Lung Deposited Surface Area
NAO	Non-Asbestos Organic
NEDC	New European Driving Cycle
PCA	Principal Component Analysis
PM	Particulate Matter
PM10	Particles with diameter $\leq 10\mu$m
PM2.5	Particles with diameter $\leq 2.5\mu$m
PMP	Particle Measurement Programme
PSD	Particle Size Distribution
SEM	Scanning Electron Microscopy
SLPM	Standard Liter Per Minute
UFP	Ultra Fine Particles (Particles with diameter $\leq 0.1\mu$m)
WHDC	Worldwide Harmonised Heavy Duty Emissions Certification
WLTP	Worldwide Harmonised Light Vehicle Test Procedure

Contents

List of Figures

List of Tables

1

Introduction

1.1 Background

Particles emitted due to road transport activities can be classified according to the source as exhaust and non-exhaust traffic-related particles [1]. Exhaust emissions occur due to the incomplete combustion of fuel or the volatilisation of the lubrication oil. On the other hand, non-exhaust particles are either generated from non-exhaust traffic-related sources, like brakes, clutch, tyres, etc or already exist in the environment as deposited materials and become re-suspended due to traffic-induced turbulence [1]. This study will focus on the latter, specifically, brake wear emissions. Brakes are a pivotal system for all road vehicles and the two configurations widely used in modern vehicles are disc brakes (Fig 1.1) and drum brakes (Fig 1.2). One of the major drawbacks of both systems is that they emit particles during the braking process, which is harmful to humans. However, drum brakes emit fewer brake particles compared to disc brakes. Due to enhanced braking performance, good heat dissipation which reduces the risk of brake fade and shorter stopping distances, disc brakes are preferred over drum brakes.

Numerous studies have reported that exhaust and non-exhaust traffic-related sources contribute almost equally to total traffic-related PM10 emissions. Due to the continuous reduction of exhaust emissions, it is expected that the contribution of non-exhaust sources will continue to increase in the coming years [1].

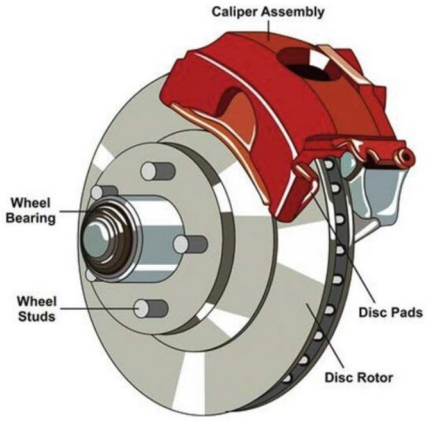

Figure 1.1: Sketch of floating caliper disc brake [2]

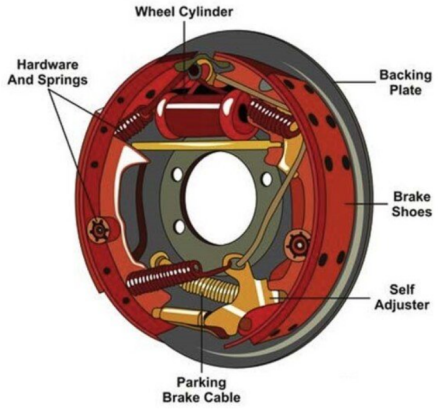

Figure 1.2: Sketch of drum brake [2]

1.1.1 Brake wear particles

The brake wear particles are classified into three main categories based on the size of the diameter of the particles as shown in Fig 1.3. Particles with a diameter less than or equal to 10μm are classified as PM10, while particles with a diameter less than or equal to 2.5μm are classified as PM2.5. Lastly, the particles with a diameter of less than or equal to 0.1μm (or 100nm) are called Ultra-Fine Particles (UFP).

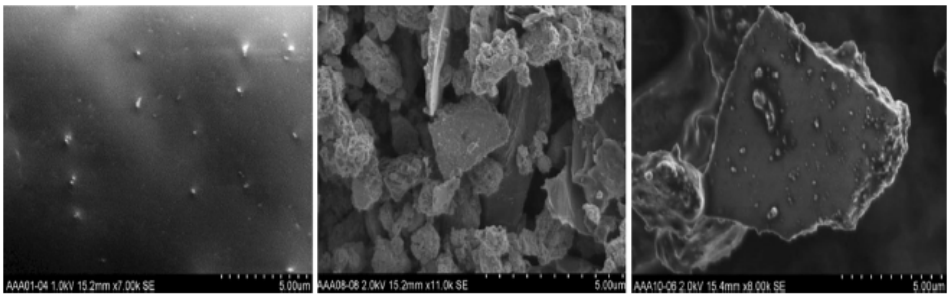

Figure 1.3: SEM images of brake wear particles (dia<56 nm (left), PM2.5 (middle), PM10 (right))[1][3]

1.1.2 Effects on human health

There are extensive studies on health risks related to airborne particles from traffic. UFP with a diameter of less than 100 nm is the current focus [4]. One of the primary causes is that ultra-fine particles enter the lungs deeply, while coarse particles end up in the upper respiratory system (the nose and throat) [1]. Other studies have shown that ultra-fine particles may become blood-borne and move to other tissues such as the liver, kidneys, and brain [1]. The same study states that the chemical composition can also greatly influence and adversely affect human health. Negative effects have been attributed to a number of PM2.5 elements that are linked to black carbon, the most significant of which are metals, inorganic salts, and PAHs (Polycyclic Aromatic Hydrocarbons) [5]. According to the World Health Organization, lung cancer, cardiovascular and respiratory disorders, as well as mortality from these

conditions, are among the harmful health effects of particulate matter that result from exposure over both short- and long-term periods [5]. Also, researchers have pointed out the long-term cardiovascular risks [1]. Overall, it is essential to monitor, regulate and control air pollution, especially in urban areas and places where people live close to the roads.

1.1.3 Euro 7 legislation

For the first time worldwide, new legislation has been framed by the European Commission to tackle/regulate the problems caused by non-exhaust emissions from vehicles. The Euro 7 standards aim to make cars cleaner and improve air quality, safeguarding both the environment and human health [6]. Euro 7 will limit the PM10 emissions coming out from the brakes of light-duty vehicles (M1/N1 category) to $7mg/km$ until 31 December 2034 and $3mg/km$ from 01 January 2035. The expected implementation date is 01 July 2025, but there might be a delay due to the ongoing discussions. Similarly, PN limits are also under consideration, but nothing has been decided to date.

To develop a system for measuring the particles that are being emitted from both light-duty vehicles and heavy-duty engines, the Particle Measurement Programme (PMP) was created. Tests are done repeatedly with different driving cycles like WLTP and WHDC to determine the emissions according to the vehicle characteristics. To make sure the emissions are within the legislation limits, test systems for brake emissions as shown in Fig 1.4 are built to do proper tests and determine the quantity of particulate matter being emitted under different driving conditions. It is vital for vehicle manufacturers to make sure their vehicles stay under the limit or they will be banned from selling in the EU. The main aim of the thesis is to set up one such system (a brake rig) and do tests under different operating conditions on a disc brake of a light-duty vehicle. The setup for this brake wear emission project is shown in Fig 1.5.

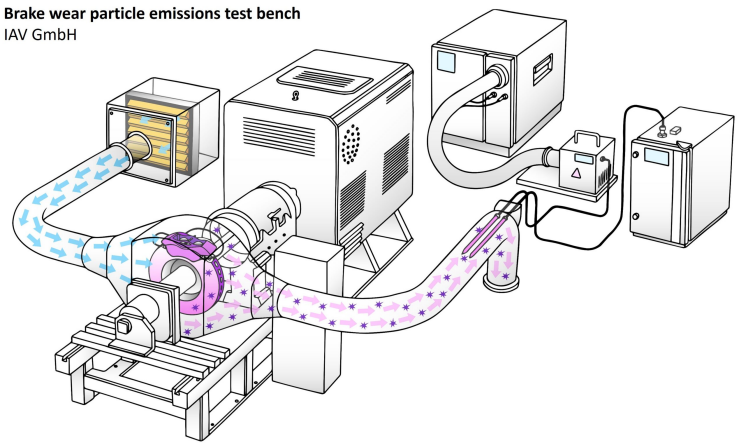

Figure 1.4: A sampling test system for brake wear emissions [7]

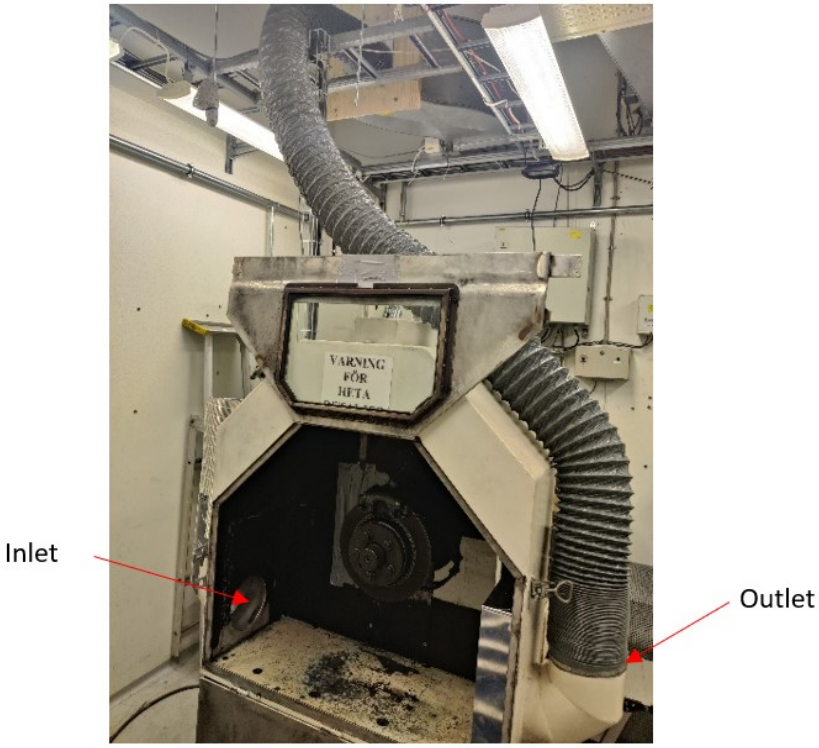

Figure 1.5: Rig used for this thesis project

1.2 Purposes

The major steps to complete this thesis project are as follows:

- Set up the brake rig for testing
- Write a program to control the rig using LabVIEW
- Study the particle size distribution
- Perform chemical characterisation of the brake dust
- Obtain accurate temperature measurements from the rig

1.3 Goals

The main aim of the thesis is to experimentally analyze the properties and composition of brake wear particles under various operating conditions of brake discs in light-duty vehicles concerning various drive and deceleration cycles. It involves setting up and assembling a fully functional brake rig for the above-mentioned aim, and programming the control system interacting with the sensors and power dynamic system for it to be run under different conditions.

2

Theory

This chapter aims to give extensive insight into brake wear particles, their formation, characteristics, measurements and health effects. The general distribution and composition of brake particles will be explored along with their environmental and health effects. Moreover, the different types of brake pads and the materials used in brake pads are also discussed. Finally, the particle sampling device ELPI and analysis methods are explained briefly.

2.1 Formation of brake wear particles

To control the vehicle speed and adapt to road conditions, the braking system is of extreme importance. With each braking cycle, wear particles are formed and released into the atmosphere [8]. The tribological characteristics of the brake system's friction couple (the brake pad's material and disc or drum brake) determine a car's brake performance, and variables like humidity, temperature, and other environmental conditions directly affect how well the brakes work [9]. However, the most responsible factors for particle formation are the initial speed, braking pressure and the achieved temperature while braking [3][8].

With the application of brakes, friction between pads/linings and rotating counterparts leads to the release of wear particles. Particles of different sizes are produced by the frictional contact between the pad and the disc. The caliper applies mechanical force to the pad during a braking event, causing it to glide against the disc and convert the vehicle's kinetic energy into thermal energy. In addition to mechanical abrasion, car brakes experience significant frictional heat generation, which leads to rotor and lining wear. Both micron-sized particles and ultra-fine particles are produced by this. The coarse particles that have not been ejected might get transferred to the brake pad and cause further problems [10].

The materials used in brake pads consist of friction modifiers, abrasives, reinforcements, fillers and binder material. According to the percentage share, the shape and size will greatly affect the braking material's tribological performances [9]. It has been found that ultra-fine particles mainly originate from the brake pads whereas the coarse particles come from the disc (cast iron in most cases) [1]. The comparison of sizes of brake wear particles (BWP) in contrast with hair and beach sand is shown in Fig 2.1.

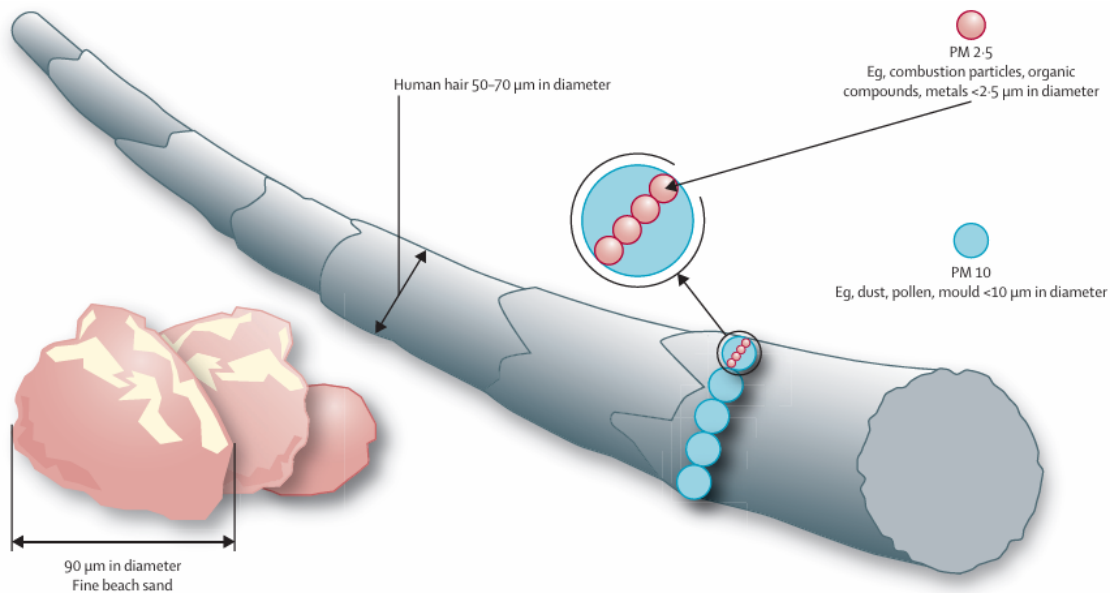

Figure 2.1: Brake particles in comparison with a strand of hair and fine beach sand[11]

2.1.1 Distribution of wear particles

A recent study shows that the majority of the road dust was generated from tyre wear at 33% followed by road dust re-suspension (31%), brake wear (19%) and exhaust emissions at 17% whereas the low contribution of exhaust PM10 emissions is because the registered vehicle models were recently made and are equipped with efficient exhaust PM reduction technologies [12]. According to several studies, brake wear can account for up to 21% of total traffic-related PM10 emissions and up to 55% of non-exhaust traffic-related PM10 emissions in urban environments while the contribution is lower in freeways and motorways because of less frequent braking [1].

When compared to larger particles, SEM images have shown that ultra-fine and some tiny particles in BWP have less sharp edges and a smoother appearance, suggesting mechanisms related to thermal and/or chemical processes [1][13]. The brake lining materials may have worn down at the brake/rotor interface due to the high temperatures. A test study has found that 86% of the brake wear airborne particle mass was distributed in the PM10 and 63% of the brake wear airborne particle mass was distributed in the PM2.5 [1][14]. In diameters smaller than 0.1 μm, wear particles accounted for about 33% by mass, which is a significant proportion of UFP. A different study has stated that depending on the type of brake pad, PM10 contributed between 63 and 85% of the total brake wear mass [1][15]. According to another report, three different NAO pads produced around 56–70% of the total brake wear mass that was released as PM2.5, and 95–98% was released as PM10 [16]. Fig 2.2 shows a typical particle size distribution.

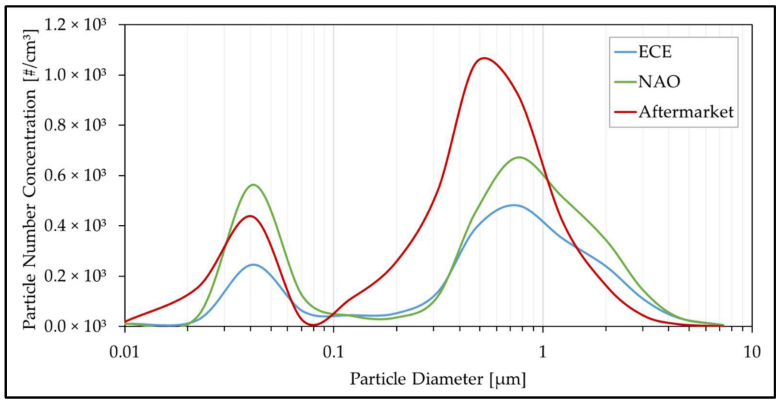

Figure 2.2: A typical particle size distribution for different types of brake pads[17]

2.2 Health effects - A bigger picture

2.2.1 Materials in brakes

Most of the brake rotors used in passenger cars are made of grey cast iron. Brake linings consist mainly of five components: binders, frictional additives, fibres, fillers and abrasives. Binders hold the components of the brake pad together ensuring structural integrity and are usually made of modified phenol-formaldehyde resins [1]. The same review study explains that the reinforcing fibres provide mechanical strength and structure to the brake lining. It can be classified as metallic, mineral, ceramic or organic and mainly consists of copper, steel, brass, potassium titanate, glass, organic materials and Kevlar. Fillers are used to reduce manufacturing costs and to improve thermal and noise properties and consist of inorganic compounds (like barium and antimony sulphate, magnesium and chromium oxides), silicates, ground slag, stone and metal powders [1]. Frictional additives or lubricants influence the wear characteristics and can be organic, inorganic or metallic materials like graphite, ground rubber, carbon black, cashew nut dust and antimony trisulphide. Finally, the abrasives are used to enhance friction, keep the contact surfaces clean and restrict the buildup of transfer films. They are usually made of Aluminum oxide, iron oxides, quartz and zircon [1]. The proportions of the materials used vary according to the type of brake lining and also, the manufacturer.

Three common lining types are non-asbestos organic (NAO), semi-metallic and low metallic. NAO pads are soft and exhibit low brake noise compared to others. But as the temperature rises, they lose the braking capacity and produce more dust relative to the other types. Earlier, brake lining consisted of asbestos but owing to the serious negative health effects, they are asbestos-free [18]. Low-metallic pads consist of organic compounds mixed with small amounts of metals and exhibit high friction and good braking capacity at high temperatures [1]. Semi-metallic brake pads have higher metallic content (up to 65% by mass), which makes them more durable and have excellent heat transfer characteristics, but tend to wear down the rotor faster and exhibit noise characteristics.

2.2.2 Composition of BWP

Due to the complex compositions of materials used in brakes, it is hard to exactly state what is being released as BWP and so is the impact on the environment [3]. The metals that we found to be in abundance despite a wide variety of materials being used according to the researchers are Fe, Cu, Zn and Pb [1][3]. Other metals like Ba, Mg, Mn, Ni, Sn, Cd, Cr, Ti, K and Sb have also been found in concentrations lower than 0.1 wt.% [3][19]. Brake linings contain 1–5% Sb in the form of stibnite (Sb_2S_3), which is used as a lubricant to reduce vibrations and improve friction stability and brake wear emissions have been found as an important source of Sb [1].

A brake dynamometer study stated that fine brake wear particles mainly comprise Fe, Cu, Ti, and Al as well as oxygen and carbonaceous species [13]. The same study mentioned that coarser particles appeared as flakes and consisted mainly of Fe in the form of its oxides and concluded that the particles were generated mechanically, suggesting brake disc wear. Also, Ti, Cu, and Al were present in some of the coarse particles, which were identified as originating from the brake pads. It was reported that metallic and carbonaceous materials constituted the finest brake particles [3]. An average element percentage in total PM10 mass of 72% with Fe, Cu, Ti, S and Zr being the most abundant was also reported [14].

2.2.3 Health significance

When taking the health effects of brake wear particles into account, particle size and chemical composition are important. The influence of particle size and how far they can go into the human body is depicted in Fig 2.3. These particles, no matter the size, cause inflammation and oxidative stress [1]. The presence of ultra-fine particles was found in the brains of animals, making it a bigger issue. Brake wear particles have a significant percentage of particles with sizes smaller than 100 nm and raise concerns of having broader health effects.

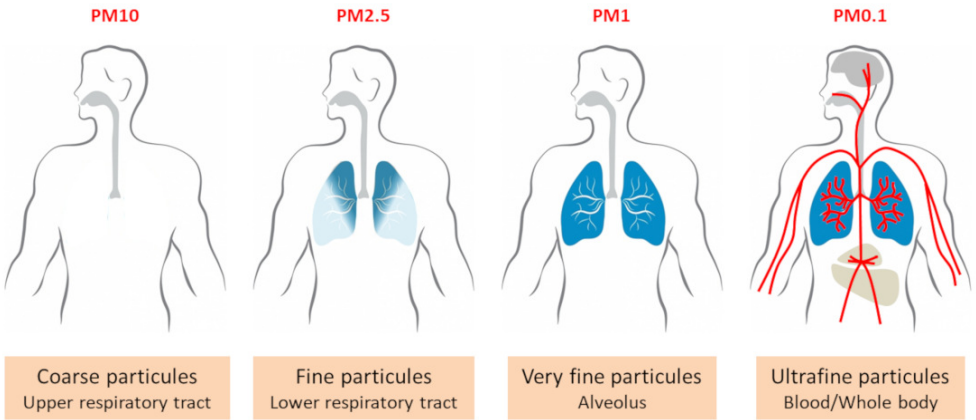

Figure 2.3: A representation of how deep PM goes into the human body [20]

Due to their ability to cause oxidative stress in biological tissues by generating reactive oxygen species, transition metals including Fe, Cu, Ni, and Cr are deemed significant with regards to their chemical composition, and metals like Zn, Al and Pb can have an influence on the effect of the mentioned transition metals [1]. The same study has highlighted how a metal causes specific health complications like Pb being linked with cardiovascular mortality and medical conditions, while Cu and S are related to monthly death rates. Also, metals like Zn, Fe and Ni in PM2.5 lead to short-term deaths, whereas Mn, Pb, Ca, Zn, Ti, Cu, Fe and V are found to be linked with daily mortality. Zn in UFP has been found to cause asthma in children on a large scale, while Fe and Se have been associated with lung inflammation [1]. The majority of these metals are present in significant amounts in airborne brake wear particles, as demonstrated by several studies, and it cannot be ruled out that these particles could have a negative impact on human health.

2.3 Particle measurement programme

Under the direction of the Group des Rapporteurs de Pollution et Energie (GRPE) of the United Nations Economic Commission for Europe (UNECE), the Particle Measurement Programme (PMP) was created to find potential systems for measuring ultrafine particles released by heavy and light-duty vehicles [21]. The objective is to create a novel measuring method that has the potential to either supplement or replace the current particle mass measurement system.

In the beginning, the main aim was to study and regulate the emissions from engines. But with the introduction of electric vehicles, the new Euro 7 puts a bigger emphasis on non-exhaust emissions. WLTP brake cycle is being used to find brake wear emissions from brakes (both pads and discs) under the desired operating conditions on test rigs or dynamometers. Several task forces have been created so as to facilitate laboratory testing and bring out constant updates/changes to the legislation that is to be mandated. Once the Working Party decides on an optimal limit for non-exhaust PM emission and Particle Number (PN) values for both light and heavy-duty vehicles, all the vehicle manufacturers will be required to comply from the release date of the legislation. Several PMP meetings are held yearly to discuss the progress and determine the modifications that need to be made to the legislation.

2.4 Electrical Low Pressure Impactor (ELPI+)

The Electrical Low Pressure Impactor is an established tool for measuring the concentration and particle size distribution in real-time in the 6 nm–10 μm particle size range [22]. The brake particles emitted are collected and sampled using a 14-phase cascade impactor according to their aerodynamic size. There is also a filter stage and a precut impactor stage (Stage 1) which usually will not have any particles deposited on it [23]. The sketch of components and how ELPI+ works is shown schematically in Fig 2.4. The ELPI+ uses a 10 Hz sampling rate to monitor particles. They are size categorised in the cascade impactor into 14 size fractions. With

the High-Resolution ELPI+ software, which uses an inversion calculation based on the actual stage collection efficiency, the ELPI+'s size resolution can be enhanced to 500-size bins instead of the regular 14 bins [22]. The principle with which ELPI+ operates consists mainly of three phases: charging the particles, followed by the inertial size categorisation in the cascade impactor and using sensitive electrometers, the particle charge is detected electrically. The particles which flow in through

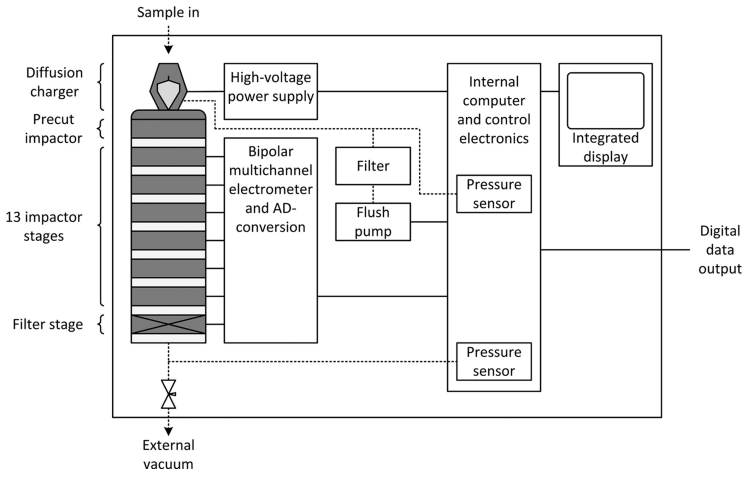

Figure 2.4: Components and operating principle of ELPI [23]

the sampling pipe into the impactor are first charged up to a known voltage level using a corona charger. The particles are categorized based on their inertia such that larger particles accumulate on the upper impactor stages, while smaller particles get deposited on the lower stages. Notably, every impactor stage is connected to an electrometer and is insulated electrically from the others. The electrometers then measure the charge carried by the charged particles as they accumulate in the various impactor stages. The number of particles is directly correlated with this measured current output [22]. The average diameters of particles measured in each stage are shown in Fig 2.5.

Stage	D50% [µm]	Di [µm]
15	10	
14	5,3	7,3
13	3,6	4,4
12	2,5	3,0
11	1,6	2,0
10	0,94	1,2
9	0,60	0,75
8	0,38	0,48
7	0,25	0,31
6	0,15	0,19
5	0,094	0,12
4	0,054	0,071
3	0,030	0,040
2	0,016	0,022
1	0,006	0,010

Figure 2.5: Different stages with respective diameters of particles measured

2.5 Characterisation methods

2.5.1 Scanning electron microscopy

Scanning Electron Microscopy (SEM) is high magnification surface morphology imaging [24]. It can be considered a useful technique for analysing materials on the nano-scale to micrometer (μm) scale, both organic and inorganic [25]. SEM mainly consists of an electron gun, a column for the electrons to travel which is equipped with multiple electromagnetic lenses, a deflection system of coils, electron detectors for the scattered and secondary electrons, a chamber to hold the sample in place and a computer to display the images and also to control the setup. The surface of the sample is examined using a concentrated electron beam at about 100 - 30000 electron volts. The spot size or the diameter of the electron beam at a certain distance from the source (an electron gun) makes it difficult to produce a sharp image of the specimen. So, lenses compress it and then direct the electrons to the specimen [25]. Different signals are produced by the interaction of electrons with the material, such as back-scattered electrons and secondary electrons[24]. The signals are then displayed on the screen and characteristics like brightness can be adjusted accordingly using the control system.

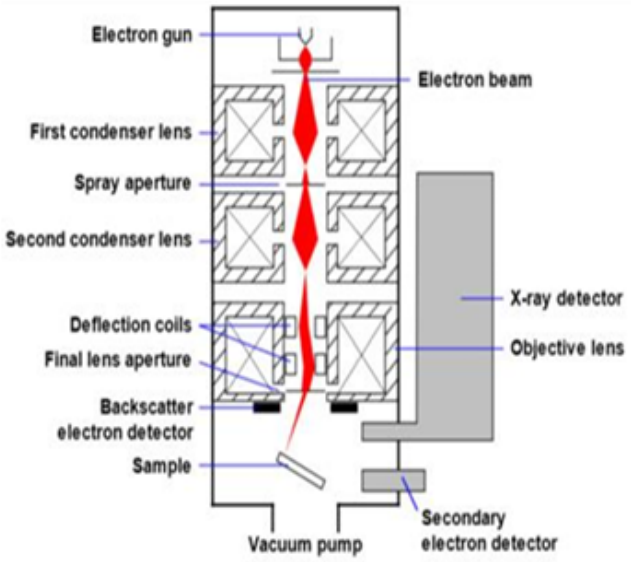

Figure 2.6: Schematic of a scanning electron microscope [25]

2.5.2 Energy-Dispersive X-ray Spectroscopy

Together with SEM, Energy-Dispersive X-ray spectroscopy (EDX) yields qualitative and semi-quantitative data. When combined, these methods can provide basic details on the material breakdown of specimens that are not possible to obtain from standard laboratory testing [25]. The tabletop SEM used for analysis is shown in Fig 2.7.

Figure 2.7: Tabletop SEM- Phenom ProX

It is essential to consider that each atom has a distinct number of electrons that are located at distinct energy levels to comprehend how these X-rays are produced [26]. These positions fall into specific shells under typical circumstances, each of which has a distinct energy. When an electron beam strikes an atom's inner shell, it removes one electron from the shell and leaves behind a positively charged electron hole, which is how EDX analysis is done as shown in Fig 2.8. An additional electron from an outer shell is drawn to the displaced electron to fill the vacuum. An X-ray can be produced when an electron transitions from the atom's outer, higher-energy shell to its inner, lower-energy shell. The energy of this X-ray is unique to the specific element and transition. A silicon drift detector collects the X-rays released during the process, measures the signal, and uses software to analyse it [26].

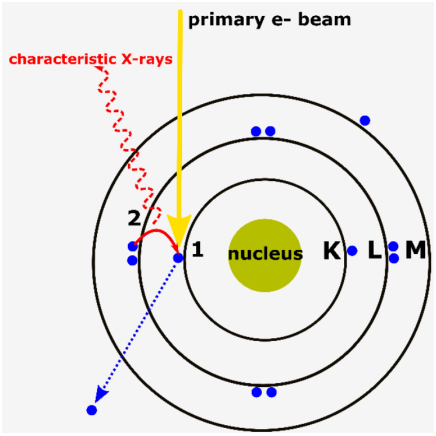

Figure 2.8: Atom and k-shell of an element during EDX [26]

3
Methodology

The thesis involved setting up a brake rig, followed by the collection and assessment of brake wear particles. This chapter details the methods by which the experimentation was carried out along with the particle measurement technique.

3.1 Test setup

The brake system used for the project is shown in Fig 3.1. The brake disc used for testing is an aftermarket disc from Biltema (Item no: 64-387). It is a plain solid cast-iron disc with a diameter of 280 mm and a thickness of 9 mm and is usually used in Ford cars and Volvo models like the C30. The brake pads used are also from Biltema and are asbestos-free (Item no: 65-001). These are mainly used in Volvo cars and are depicted in Fig 3.2.

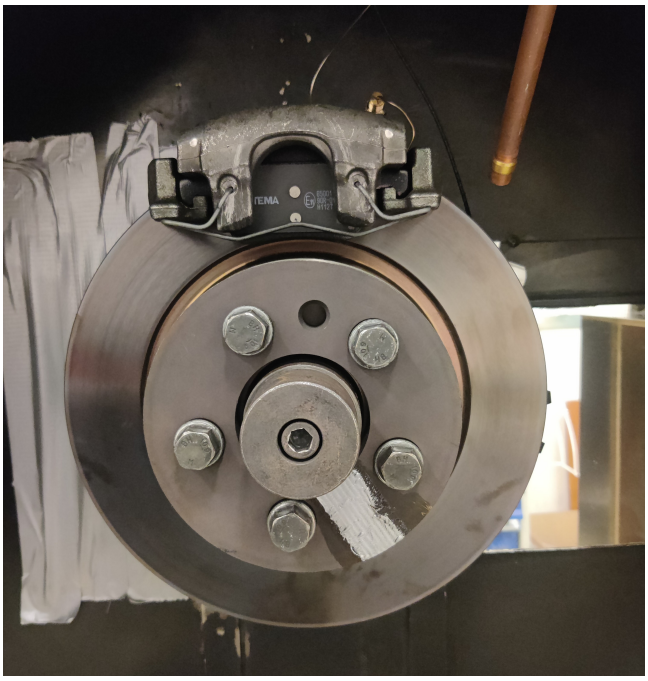

Figure 3.1: Brake assembly

Figure 3.2: Brake pads used in the investigation

3.1.1 Overview

The test setup was done in a test cell using limited resources available at the Energy Conversion and Propulsion Systems (ECaPS) division at Chalmers. An old dynamometer was used for tests to generate brake particles while collecting them simultaneously. The inertia of the rig is about $30kg.m^2$. The software used to control the rig and get measurements is LabVIEW. A computer is connected to the NI Compact RIO chassis via an ethernet cable which then provides input to the variable frequency drive and actuates the brake according to the braking input. The brake system is controlled using a brake unit, which in turn is controlled using the electronic proportional valve driver. The input signals were given using a LabVIEW program specifically made for this system. The brake unit consists of a pressure sensor, pump, ON/OFF valve and a proportional valve. The layout of the whole system is depicted in Fig 3.3.

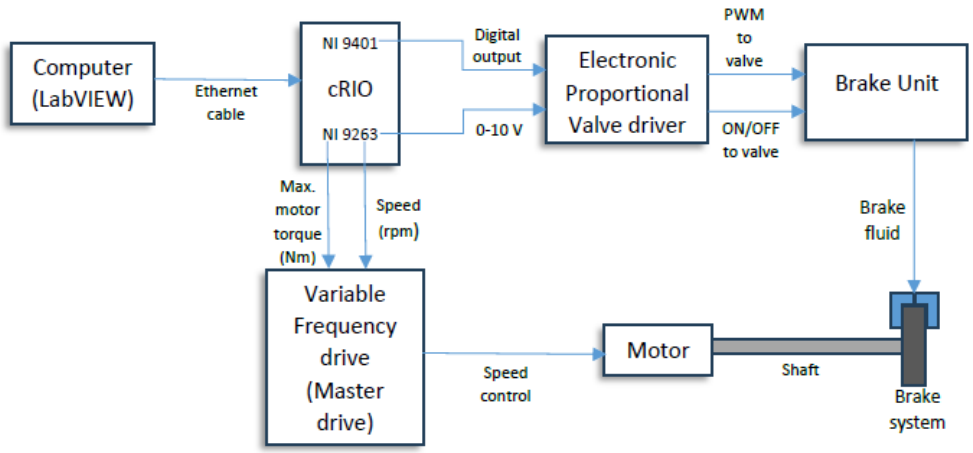

Figure 3.3: System layout

3.1.2 Limitations

The main aim of this thesis is to analyze the brake wear particles and their composition. Due to time constraints and delays in getting parts delivered, a temporary setup was made to generate brake particles. As a result, heavy braking could not be done as the temperature was too high for the brake system to withstand due to lack of proper cooling. Due to this, standard test cycles like WLTP, FTP-75, NEDC, etc could not be run and a custom test cycle was created to carry out the tests along with different brake pressures. Also, due to the lack of an air circulation system in place, a strong ventilation system for the room was used to create an airflow inside the brake enclosure at a rate of approximately 5262 slpm.

3.2 Test cycle

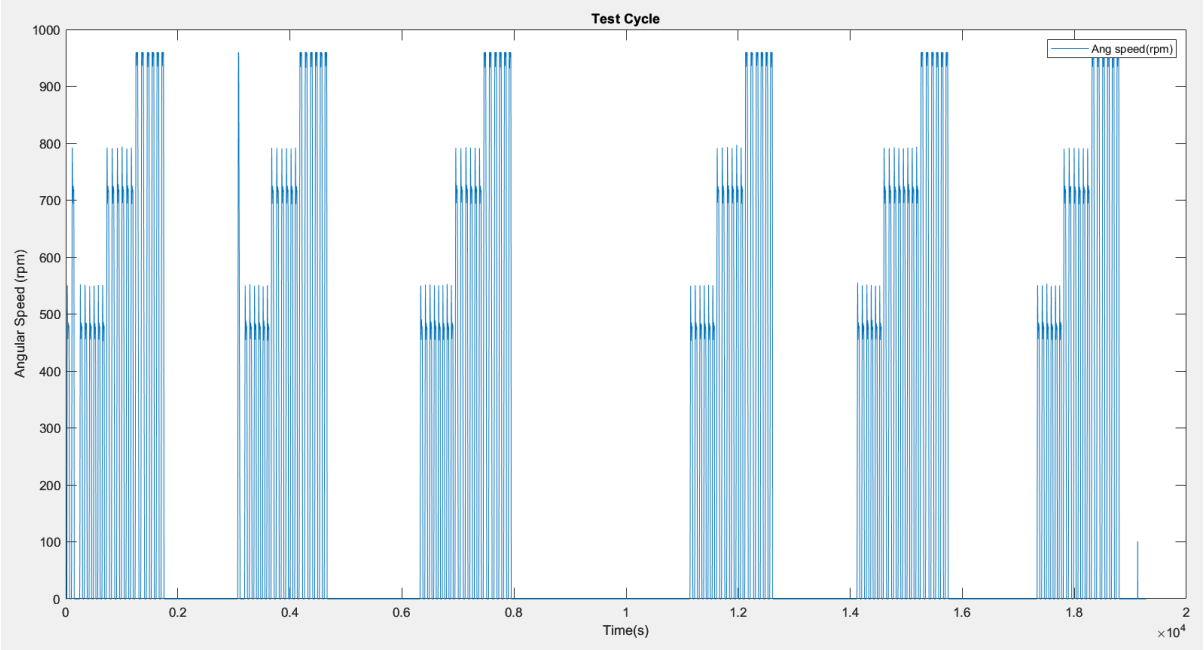

Figure 3.4: Test cycle for analysis of brake wear emissions

The test cycle used in this project is shown in 3.4. It is custom-made and suitable for the working conditions of the brake rig. It is set such that each set of data (Table 3.1) entered is run twice followed by a gap of 30 seconds. The brake pressure peaks at 28% for the system and is used for the last run for each speed. In addition, the test cycle is designed to study the properties of re-suspension of brake particles, in a way that there is adequate time for the brake disc and brake pads to cool down for the repeatability of the tests.

The brake disc is accelerated quickly to a maximum speed of 960 rpm a few times. To generate the maximum amount of particles under the restraints, two other speeds of 480 rpm and 720 rpm are also used followed by a braking-to-zero braking event

from these set speeds. These events are repeated at fixed intervals while collecting particles for sampling.

Table 3.1: Various brake pressures and shaft speeds used for testing

Angular speed (rpm)	Brake pressure (bar)
480	18
480	38
480	54
720	18
720	38
720	54
960	18
960	38
960	54

3.3 Braking parameters

Basic parameters like angular speed, torque, brake temperature and pressure are acquired from the brake rig. Knowing the maximum torque is 2400 Nm and the maximum speed is 250 km/h for the rig, the corresponding speed in km/h can be calculated using angular speed.

3.3.1 Data pre-processing

Due to some delay in getting the brake unit to apply brakes instantly, the brake pressure had an error of 1.799 bar throughout the experiment even after calibration. It is the difference between the measured value and the actual set value. Owing to this, the error factor has been subtracted from the data to get more accurate results. Noise signals in all of the parameters have been removed by cleaning the data by setting all the negative values to zero where the values should have been non-negative and also by setting a threshold value of 5% of the maximum value.

3.3.2 Brake events

Braking events need to be identified to analyze the braking characteristics per event. Due to a lot of noise signals from the data acquisition system, a backtracking method is used to identify the start point of all the brake events since the endpoints of all braking events are at 0. Hence, the start point of a braking event is set to be the highest and closest peak before the angular velocity goes to 0. A braking event is shown in Fig 3.5. There are 114 braking events for the test cycle.

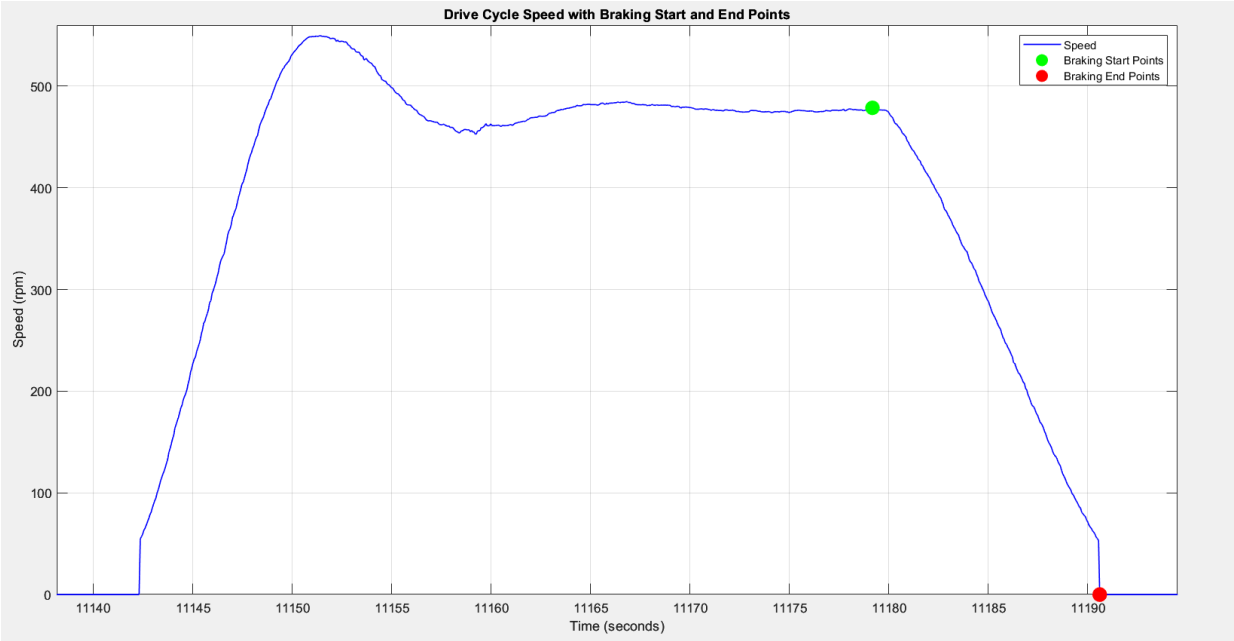

Figure 3.5: A snippet of one braking event

3.3.3 Brake energy and power

3.3.3.1 Brake power

The angular velocity (ω) of the disc and braking torque (τ) produced are recorded. Using these, the brake power in Watts is calculated using equation 3.1 which is later converted to kW. The brake power curve for a brake event is shown in Fig 3.6.

$$P_{brake} = \tau\omega(\frac{2\pi}{60}) \tag{3.1}$$

3.3.3.2 Brake energy

Brake energy is calculated by integrating power over time. This can be done based on the simple equation:

$$E_{brake} = P_{brake} * t \tag{3.2}$$

Equation 3.2 assumes constant power and in this case, the power is not constant. To get precise results, the MATLAB function '*trapz*', is used to calculate the brake energy. The braking energy per braking event is depicted in Fig 3.7. The first two braking events are to warm up the brake disc to a temperature of approximately 50°C, which is a feasible temperature to cool down the disc to start the next cycle quickly.

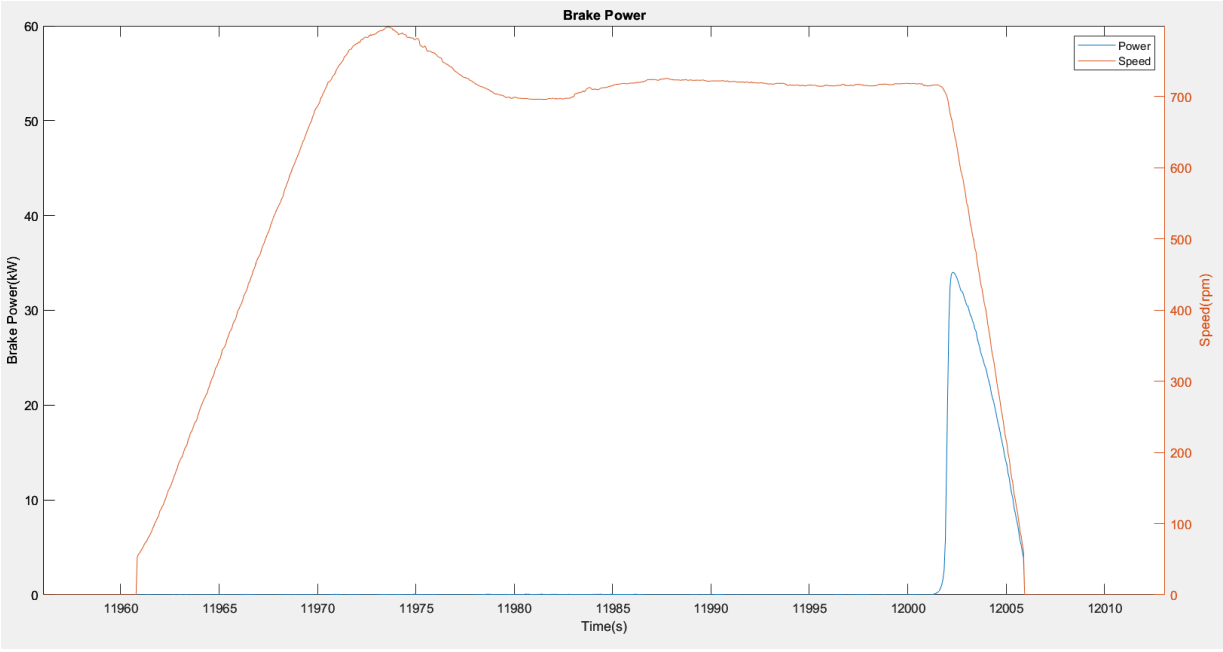

Figure 3.6: Brake power curve snippet

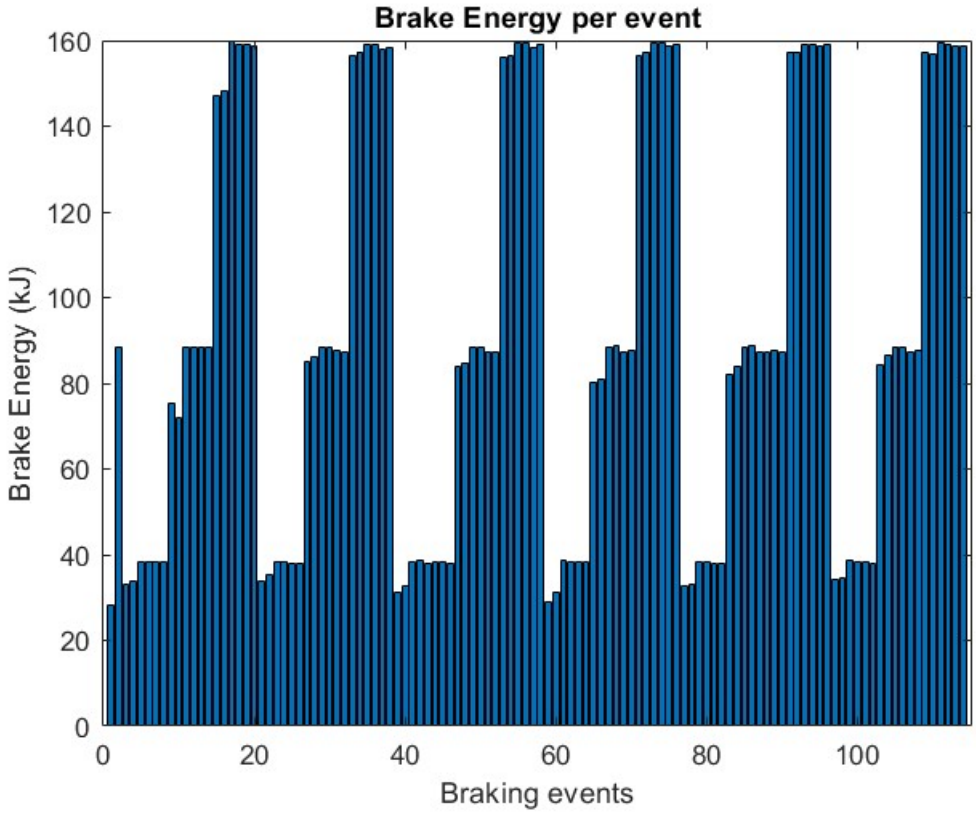

Figure 3.7: Brake energy per event for all 114 events

3.4 Brake particle analysis

3.4.1 Sampling

The brake particles were sampled using the Dekati ELPI+ impactor. A copper pipe was placed close to the brake disc right next to the brake caliper in the direction of the airflow as shown in Fig 3.8 & Fig 3.9. The exit port of the rig has a HEPA filter so that the brake particles will not get into the ventilation system and the enclosure is tightly sealed to prevent any brake dust from getting out and polluting the room.

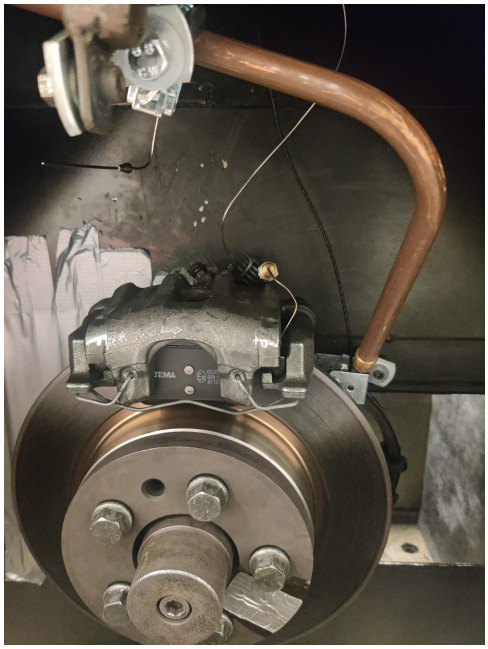

Figure 3.8: Front view of the pipe to sample brake wear particles

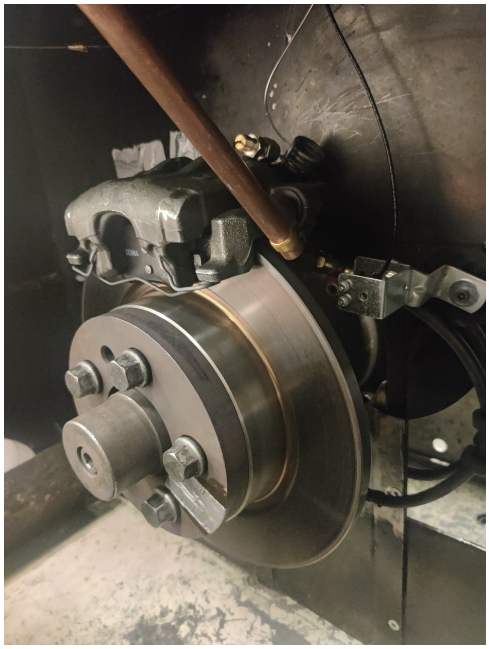

Figure 3.9: Side view of the pipe to sample brake wear particles

The brake particles are sampled at a rate of 10 L/min in the impactor. The particles get collected in the aluminium foils as shown in Fig 3.10, which are fixed on the collection plates inside the impactor which will be operated at an internal pressure of 40 mbar. The particles get deposited based on their size where the smaller, finer particles are deposited at the lower stages like 2, 3, 4 etc, and the larger, coarser particles get deposited at the top part of the impactor in stages like 10, 11, 12 etc.

Figure 3.10: Aluminium foil with brake particles from the impactor (Stage 11)

The impactor is disassembled to collect the aluminium plates for SEM analysis (Fig 3.11). Aluminium foil from each stage is stored separately as shown in Fig 3.12, and the data from the ELPI is later used to determine the stages that should be used for analysis depending on the amount and number of particles collected.

Figure 3.11: Disassembled impactor with all the impactor stages and collection plates

Figure 3.12: Al foils from all stages collected for SEM analysis

3.4.2 Analysis

The collected particles are analysed to find their composition and to visualise the structure of the brake particles at different levels. The foils are carefully mounted onto a metal stud using a double-sided carbon tape as shown in Fig 3.13. These are then placed inside the microscope followed by the projection of electrons into them, giving magnified images of brake particles at micrometer and nanometer levels. The instrument used for analysis is Phenom ProX from Phenom-World.

Figure 3.13: Aluminium foil mounted on a stud for SEM analysis

When determining the composition of brake particles using EDX, all the materials with electron energies less than 1 keV are neglected since the efficiency of element detection significantly decreases for electron energies below 1 keV. Also, materials with atomic and weight concentrations of less than 1% are ignored due to the detection limits of the machine. The x-axis consists of the electron energy values in keV and the y-axis depicts the counts and the material will be highlighted in green circles as shown in Fig 3.14. The best fitting curve is adjusted and selected manually to find the materials in the brake dust which have electron energies close to the ones that are displayed on the monitor. In the results section, the images and composition of the brake particles analysed will be explained in detail.

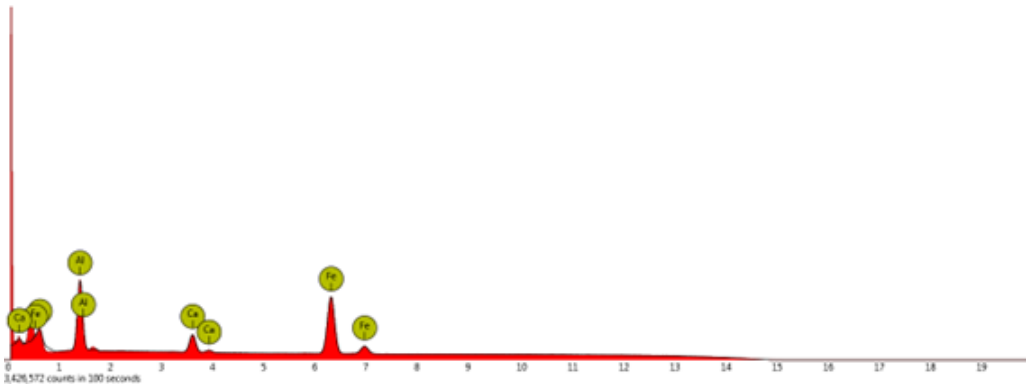

Figure 3.14: Electron energy (keV) vs Count plot from EDX analysis using Phenom SEM

4

Results

4.1 Wear characteristics

4.1.1 Brake pads

The brake pad thickness before and after the testing is depicted in Table 4.1 and Table 4.2 for inner and outer brake pads respectively. The points used for measurements are shown in Fig 4.1. For the inner pad, which is attached to the brake cylinder, the rotation of the brake disc will be in the clockwise direction whereas for the friction surface of the outer pad, the rotation is anti-clockwise. For the inner pad, points 1 and 4 are on the lead side and points 2 and 5 are on the tail side. Similarly for the outer pad, points 2 and 5 are on the lead side and points 1 and 4 are on the tail side. The lead side is typically in the direction of rotation of the disc.

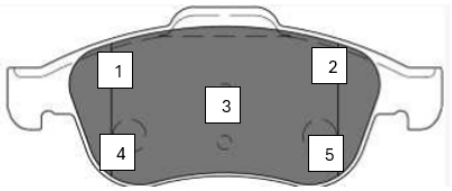

Figure 4.1: Five points where the thickness of the brake pads are measured [27]

Table 4.1: Thickness of inner brake pad before and after testing

Location	Thickness before testing (mm)	Thickness after testing (change)(mm)
1	16.46	15.56 (-0.90)
2	16.65	16.05 (-0.60)
3	16.57	15.65(-0.92)
4	16.56	15.58 (-0.98)
5	16.77	16.05 (-0.72)

Table 4.2: Thickness of the outer brake pad before and after testing

Location	Thickness before testing (mm)	Thickness after testing (change)(mm)
1	16.77	15.77 (-1.00)
2	16.74	16.02 (-0.72)
3	16.77	16.20 (-0.57)
4	16.80	15.73 (-1.07)
5	16.77	16.07 (-0.70)

The brake pad attached to the brake cylinder weighed 245.44 g before testing and 234.44 g after testing, resulting in a net loss of 20 g or 7.8 % whereas the other brake pad weighed 245.02 g before testing and 235.72 g after testing, resulting in a net loss of 9.3 g or 3.8 %. The brake pad attached to the brake cylinder experienced more wear, losing nearly twice as much as the other brake pad. For both pads, it is clear from the tables that most of the brake wear happened at locations 1 and 4. For the inner pad, these points are close to the inlet port of the rig. In the case of the outer pad, they are on the side close to the exit port of the rig, i.e., in the direction of the airflow.

4.1.2 Emission factor

From the recorded particle data, the total weight of PM10 is 6.223 mg and the total braking energy for all events is 10.636 MJ. So, the emission factor is 0.585 g/GJ or 585 mg/GJ and 0.0374 mg/km. It is well within the 3 mg/km limit for Euro 7. However, the test cycle is unrealistic and comparing the emission factor with that of the legislation does not provide much insight. The emission factor is quite low since only a small percentage of the particles produced have been sampled. Moreover, the sampling position is not optimal and the actual value will be a qualitative analysis which can be done in the future.

4.2 Particle size distribution

The particle data obtained from ELPI is merged with the braking event curve and the brake pressure curve to study the particle size distribution at different stages. A combined snippet for one braking event is shown in Fig 4.2. The particles recorded during the re-suspension and braking event are indicated in the figure. As soon as the disc starts to rotate, the brake particles get suspended in the air. It is visible that the number of particles released from the brake system increases rapidly as soon as the brake is applied. The effect of speed on re-suspension is explained with PSD curves. The particle deposition of the already formed particles continues to happen even after the braking ends, due to the rotation of the disc.

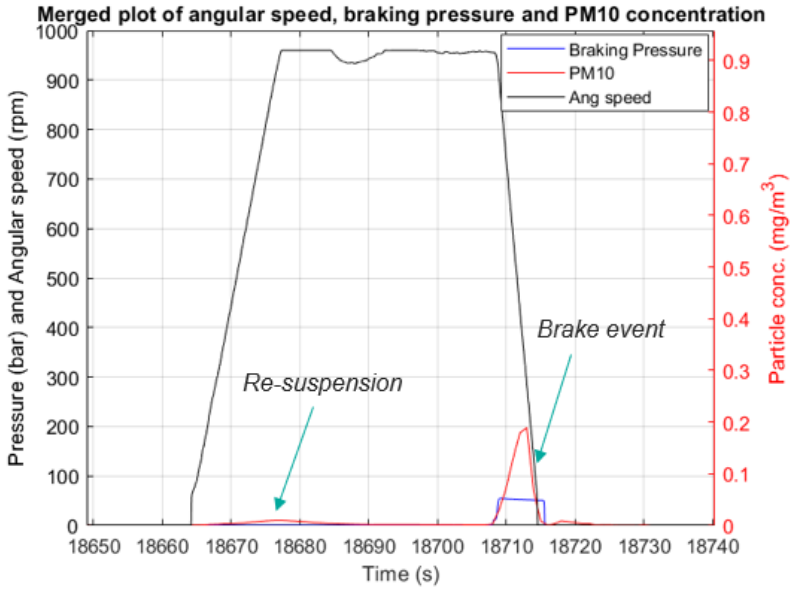

Figure 4.2: A snippet of angular speed, PM10 data and brake pressure combined

The average particle size distribution with the particle number per cubic cm and concentration of particles is plotted for the entire time frame of about 19281 seconds as shown in Fig 4.3. It can be seen that the average particle concentration is high around the PM2.5 region, which could be because of the influence of several parameters like speed, pressure and temperature during each braking event.

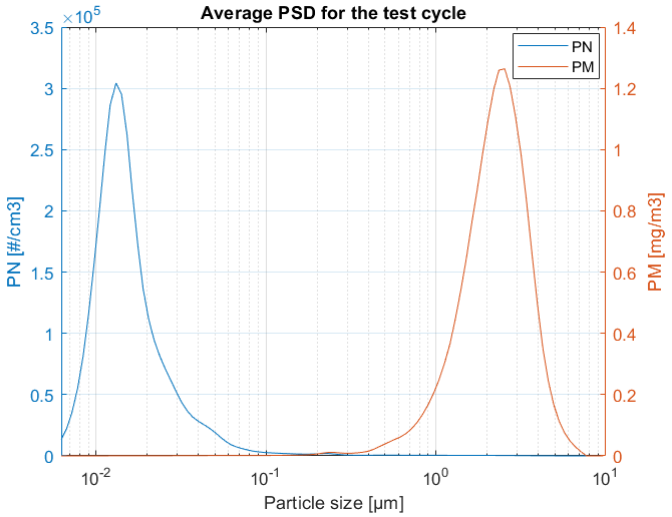

Figure 4.3: Average PSD for the test cycle

As discussed before, non-exhaust emissions can exist as deposited materials in the environment and can be re-suspended in the air. Particle size distribution for two re-suspension events at different speeds are depicted in Fig 4.4 and Fig 4.5. When the brake disc starts running after braking, the already-formed particles get suspended

in the air again, and the recorded data shows that many small particles get re-suspended. It can be seen from the graphs that at a higher speed, more particles get re-suspended into the air, with a higher concentration. However, it is not evident that the particles recorded have been re-suspended from the brake system or the base and associated parts of the brake enclosure.

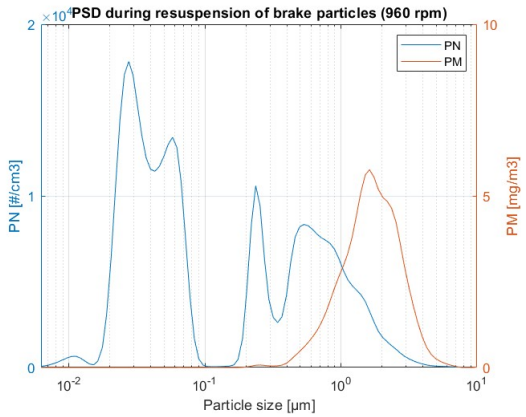

Figure 4.4: PSD during re-suspension at 960 rpm

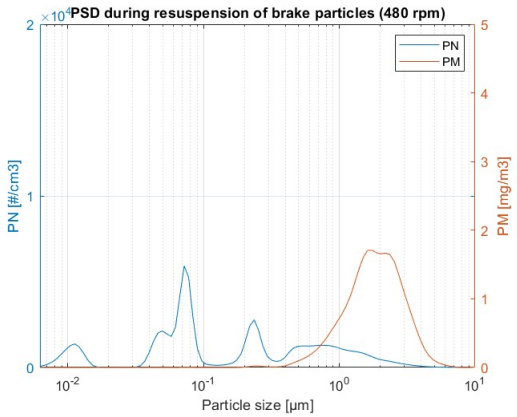

Figure 4.5: PSD during re-suspension at 480 rpm

It is important to evaluate the influence of temperature, pressure and speed on the characteristics of the particles produced. During the tests, the temperatures recorded went as high as 327°C and sparks were seen during those periods. An infrared image of an extremely hot brake disc captured is shown in Fig A.4. Three different cases for studying the effect of each parameter are made while keeping the other two constant. The particle size distribution for the effect of temperature on the brake particle formation for two different is depicted in Fig 4.6 and Fig 4.7 at 306°C and 311°C peak braking temperatures respectively. It can be seen that with an increase in temperature, more particles are produced, as evident from the PN curve. However, the difference in particle concentration of PM is huge, which is a scope for future work.

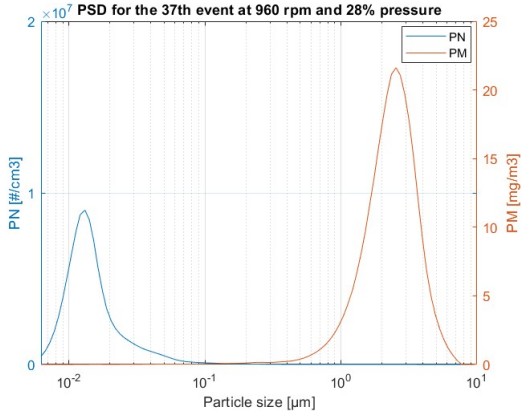

Figure 4.6: PSD at 306°C

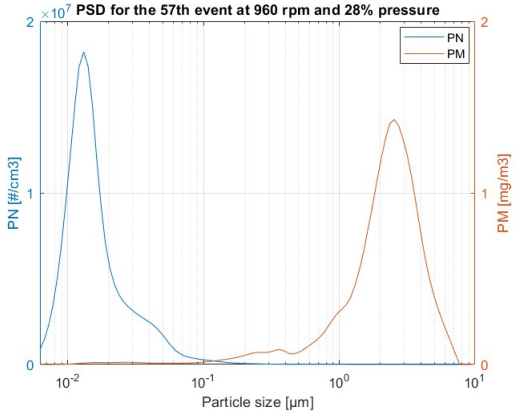

Figure 4.7: PSD at 311°C

Fig 4.8 and Fig 4.9 represent PSD at two different, yet almost similar speeds. The number concentration and mass concentration are almost identical. Fig 4.10 and Fig 4.11 show how PSD varies with varying brake pressure. From these cases, it is seen that with a slight increase in pressure, the number of particles produced decreases which could be because of several factors like reduction in friction coefficient which requires an in-depth analysis.

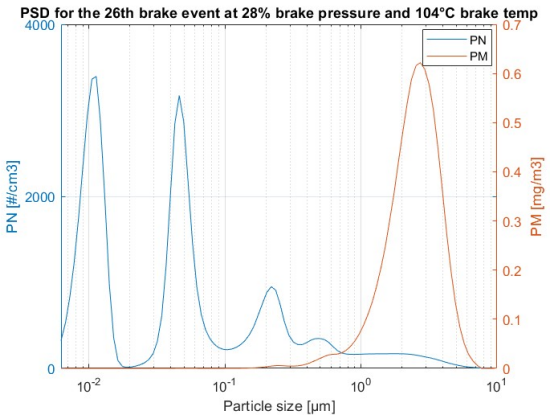

Figure 4.8: PSD at 714 rpm

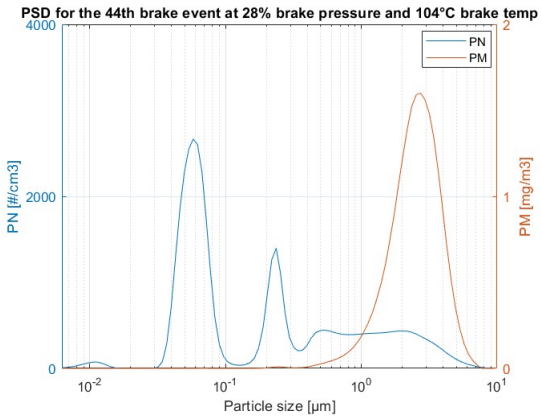

Figure 4.9: PSD at 716 rpm

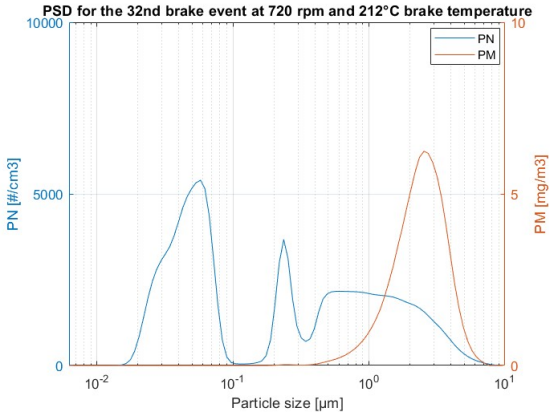

Figure 4.10: PSD at 54.7 bar brake pressure

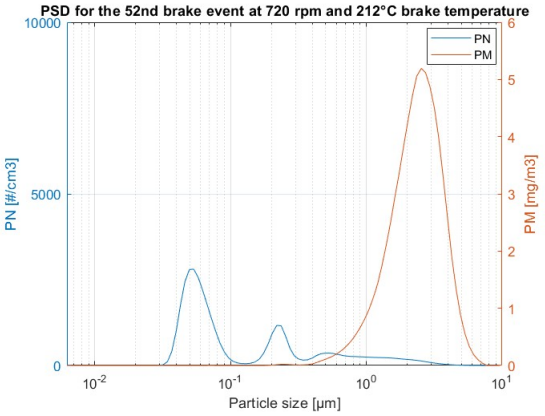

Figure 4.11: PSD at 56.3 bar brake pressure

4.3 Brake wear particles

The brake particles collected are depicted in Fig 4.12 and Fig 4.13 as PM10 and PM2.5 data respectively, which are used for further analysis.

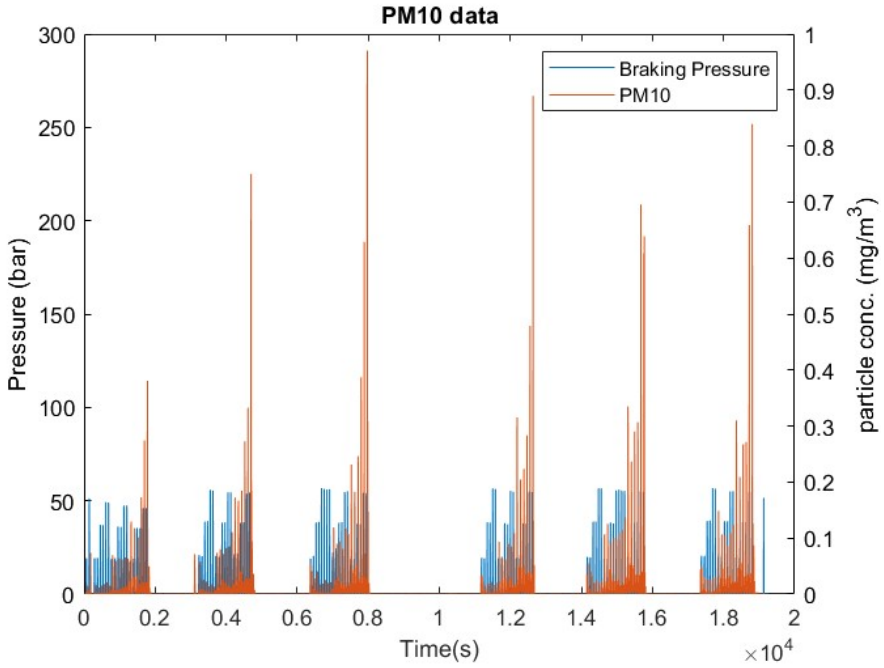

Figure 4.12: PM10 data recorded using ELPI merged with brake pressure

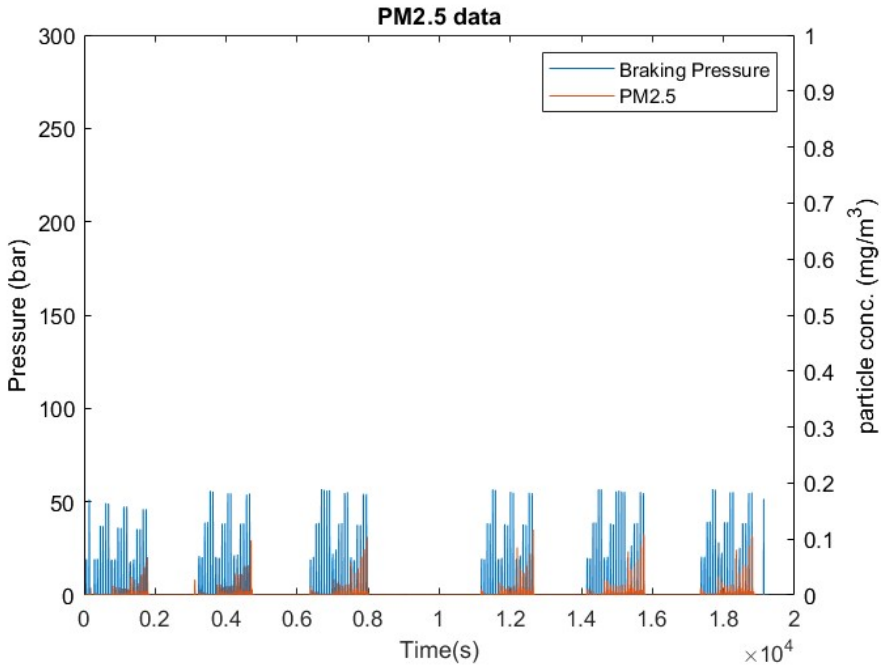

Figure 4.13: PM2.5 recorded using ELPI merged with brake pressure

A lot of brake dust has been collected and analysed for its characteristics and material composition. Microscopic images of brake particles are shown in Fig 4.14 and Fig 4.15. The images are acquired in such a way that the visual aspect as well as the quality is good enough given that the equipment had its demarcations.

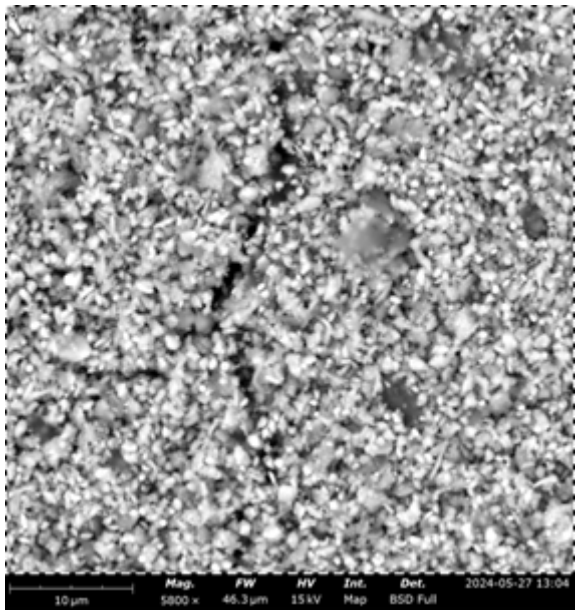

Figure 4.14: Brake particles under an electron microscope at 5800x magnification (Stage 10)

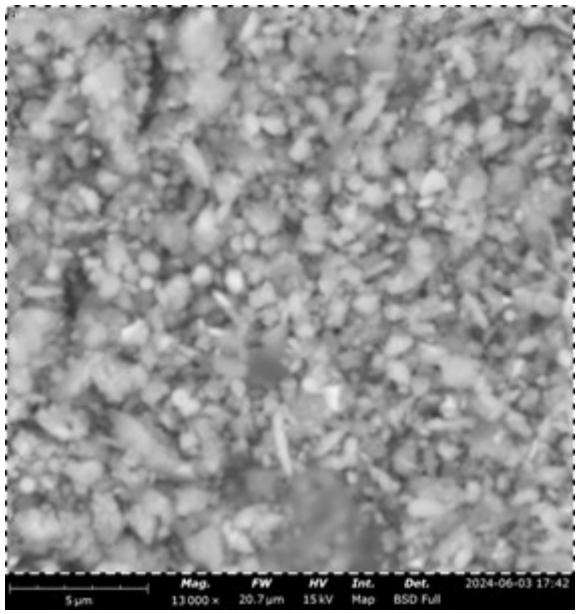

Figure 4.15: Brake particles under an electron microscope at 13000x magnification (Stage 9)

The stages 5, 7, 9, 10 and 12 were selected for analysis because of the abundance of the particles that are deposited on them and the particle concentration at different stages are depicted in Fig A.9 and Fig A.10 in the form of average PN, PM and LDSA plots for the whole test cycle. Visually and analytically, among the lower stages, 5 and 7 had relatively more concentrations of brake particles. After analysing different regions and different points of several impactor stages, the elements found are Iron, Calcium, Silicon, Aluminium, Sulfur and Phosphorous. The Phenom electron microscope cannot detect carbon hence it was not found. The metal Fe was found in abundance at approximately 90% weight concentration and atomic concentration, especially at higher impactor stages mainly because of the cast iron brake disc used for testing. At the lower levels, due to the relatively small size of the patterns of brake particles deposited on the foil, Al is found in abundance because of the Al foils used.

Due to the limitations of the Phenom microscope, a detailed analysis was carried out using an electron microscope from Oxford Instruments. The weight percentage of the elements found at different stages and areas of the Al foils are depicted in Fig A.8. The elements detected are C, O, Si, P, S, K, Ca, Mn, Fe, Cl, Cr, Ni, Th, Tb and Ag. The presence of Sb, which is usually found in brake wear particles, has not been detected. This could be because of the minute amounts of Sb in the brake pad composition and the regions analysed using SEM-EDX. Some elements like Cr, Ni, Th, Tb, and Ag are found very few times in stage 5 of the impactor and for most cases, the weight percentage is less than 1%. Thorium, a radioactive metal, might have been detected because of the overlap of electron energies with another element. For this reason, they are not considered assuming these elements might not be present. Al was excluded from the intricate analysis as well due to its interference at lower stages because of the Al foils used. The findings are explained in detail in the form of PCA plots.

4.4 Principal component analysis

Principal component analysis (PCA) is a technique used to simplify complex databases by reducing the number of variables by transforming the data into a new set of variables called principal components while retaining the original information. For the recorded dataset, PCA is carried out with PM size (the size of particles measured in different impactor stages) as the principal component to understand the correlation between PM size and the elements detected. The scatter plot helps to see the new data points in the newly created space defined by principal components. The loading plot provides the relation of the original variables to that of the principal components. In Fig A.8, the weight percentage of elements present at 41 different locations in 5 different stages is indicated and the ones with the highest percentage have been highlighted. Scatter plots for various spectra (points which were used for identification of the elements in the Al foil) are made to identify the trend in all the detected elements with the PM size. However, due to their minute presence, Cr, Ni, Th, Tb, and Ag are not used for PCA.

The scatter plot (Fig 4.16) indicates how the size of the accumulated particles varies with changing stage numbers. It highlights the clusters of all the spectra of different stages with a similar trend related to the principal component, PM size. In stages 10 and 12 (towards the left in the scatter plot), the larger PM is dominant while in the lower stages, the smaller ultra-fine particles are dominant. This is plotted with PM size as the principal component. Different spectra are marked followed by the number of the stage for which the test is done, for example, 24_#5 means spectrum 24 of stage 5 (Fig A.11 and Fig A.12) and the colour scale varies from blue for the smaller PM to red for the larger PM.

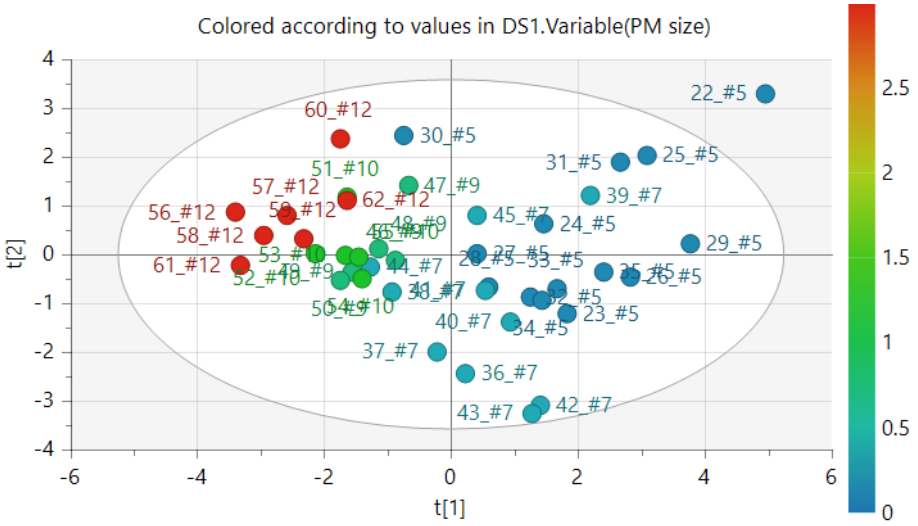

Figure 4.16: PCA scatter plot based on PM size

The loading plot (Fig 4.17), shows how each element correlates to the principal component, PM size. The closer the element is to the 'PM size' variable, the larger will be the size of it. Metals Fe and Ca constitute most of the larger PM whereas elements like C, Si, O, etc contribute the majority of the larger particles. These can be verified with all the other findings and Fig A.8, where C and O are dominant in stages 5 and 7 compared to Fe.

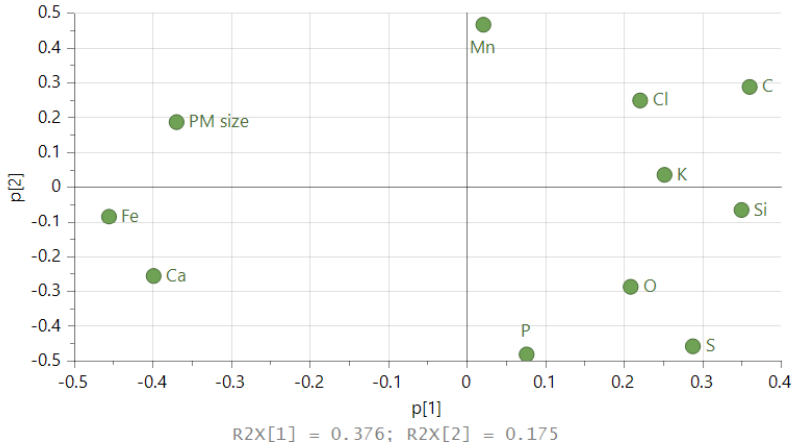

Figure 4.17: Loading plot for elements

5

Discussions and Conclusions

5.1 Discussions

This experimental study which determined the characteristics of brake wear particles has provided some basic insights into the shape, size, composition and concentration of brake particles. A single set of brake pads and a cast iron disc were tested repeatedly using a custom-built drive cycle.

The method by which the particles were recorded and measured is not effective since most of them did not go into the ELPI impactor. The total loss from the brake pads accounted for 29.3 g whereas the total mass of recorded particles is approximately 6.223 mg. With the introduction of a strong fan with an air circulation system, this problem could be eradicated since most of the particles could be sampled and the results would be more accurate. Moreover, data recording could be done without much noise in the system, especially the pressure data with a slight error. Also, the system's response to the inputs was not instant, specifically when giving the signals to start the braking action. It was also noted that activating the brake without setting the angular speed to zero produced a negative torque even after the brake disc stopped spinning, which is undesirable. To avoid this, the system is programmed to set the speed to zero right before the brake is applied.

This study does not provide an insight into why the particles produced decrease with increasing pressure for similar speed and temperature conditions. Similarly, it is not clear why the concentration of particles is different by a big margin at similar brake pressure and speed for two different cases. To get an accurate conclusion on the effect of these parameters, a more sophisticated study is required.

5.2 Conclusions

A custom drive cycle was successfully created to capture the brake particles and investigate the effects of speed, braking power and temperature on the properties of the particles released. A detailed study using a total of 114 brake events has been carried out to find how these parameters affect the characteristics of brake particles. It is found that the higher the temperature, the more the number of particles produced. The brake particles are produced by the brake system not only during the braking phase but also during the acceleration phase in the form of re-suspended particles. For the cases of particle re-suspension, the number of particles as well as

the particle concentration is dependent on the speed i.e., as the speed increases, a larger the number of particles get re-suspended in the air. For high-speed braking and high disc temperature braking cases, the number of particles emitted is high. At brake disc temperatures of $320°C$ and higher, sparks were observed and it is not good in a real-life situation. So, low disc temperatures and low-speed braking are ideal for a safer operation even though it is not practical. However, a combination of regenerative brakes and conventional braking could influence the reduction of brake particles produced per braking.

The collected brake particles were further analysed for their chemical composition to observe the shape and size of the brake particles. The results are verified with the help of PCA plots along with SEM-EDX analysis. Due to the limitations of the Phenom ProX microscope, advanced equipment from Oxford Instruments was employed to get more precise results. It was observed that the lower stages like 5 and 7 had most of the smaller PM while higher stages like 9 and 10 comprised mostly of larger PM, i.e. PM10. It is also found that metals like Fe and Ca make up most of the larger PM whereas elements like C, Si, O, S etc make up most of the smaller size PM or ultra-fine particles. These results on how the chemical composition changes with size are vital for studying the effects of brake particles on human health.

With new stricter rules coming to the area of non-exhaust emissions, effective ways to capture most of the brake particles emitted from a vehicle or ways to reduce their formation by the use of a combination of different pairs of available brake pads like metallic and semi-metallic, other brake discs or even drum brakes should be studied extensively since frictional brakes could not be replaced by regenerative braking for safety reasons.

This study on brake wear emissions is done at a basic level. It can be expanded with more sophisticated equipment, concerning the new upcoming Euro 7 standard and using the standard drive cycles. With proper cooling, ventilation and enclosure more rigorous tests and standard drive cycles could be run. Tests could also be run to determine which combination of brake pads and discs would prevent more brake wear from happening alongside the effect of regenerative braking.

References

[1] T. Grigoratos and G. Martini, "Brake wear particle emissions: A review," *Environmental Science and Pollution Research*, vol. 22, pp. 2491–2504, 2015.

[2] "Disc brakes vs Drum brakes." `https://www.spinny.com/blog/index.php/drum-brakes-vs-disc-brakes/`. Accessed online 2023-10-27.

[3] J. Kukutschová, P. Moravec, V. Tomášek, V. Matějka, J. Smolík, J. Schwarz, J. Seidlerová, K. Šafářová, and P. Filip, "On airborne nano/micro-sized wear particles released from low-metallic automotive brakes," *Environmental Pollution*, vol. 159, no. 4, pp. 998–1006, 2011.

[4] L. Bondorf, L. Köhler, T. Grein, F. Epple, F. Philipps, M. Aigner, and T. Schripp, "Airborne Brake Wear Emissions from a Battery Electric Vehicle," *Atmosphere*, vol. 14, no. 3, p. 488, 2023.

[5] "Health Effects of Particulate Matter," *World Health Organization*, 2013.

[6] European Commission, "Euro 7 standards to reduce pollutant emissions from vehicles and improve air quality." `https://ec.europa.eu/commission/presscorner/detail/en/ip_22_6495`. Accessed online 2024-02-08.

[7] IAV Global, "Brake wear particles in focus: New test benches in Gifhorn." `https://www.iav.com/en/news/brake-wear-particles-in-focus-new-test-benches-in-gifhorn/`. Accessed online 2024-02-08.

[8] N. Stojanovic, J. Glisovic, O. I. Abdullah, A. Belhocine, and I. Grujic, "Particle formation due to brake wear, influence on the people health and measures for their reduction: a review," *Environmental science and pollution research*, pp. 1–20, 2022.

[9] M. Kchaou, A. Sellami, J. Fajoui, R. Kus, R. Elleuch, and F. Jacquemin, "Tribological performance characterization of brake friction materials: What test? what coefficient of friction?," *Proceedings of the Institution of Mechanical Engineers, Part J: Journal of Engineering Tribology*, vol. 233, no. 1, pp. 214–226, 2019.

[10] W. Österle, I. Dörfel, C. Prietzel, H. Rooch, A.-L. Cristol-Bulthé, G. Degallaix, and Y. Desplanques, "A comprehensive microscopic study of third body formation at the interface between a brake pad and brake disc during the final stage of a pin-on-disc test," *Wear*, vol. 267, no. 5-8, pp. 781–788, 2009.

[11] M. Guarnieri and J. R. Balmes, "Outdoor air pollution and asthma," *The Lancet*, vol. 383, no. 9928, pp. 1581–1592, 2014.

[12] H. Al-Thani, M. Koç, C. Fountoukis, and R. J. Isaifan, "Evaluation of particulate matter emissions from non-passenger diesel vehicles in qatar," *Journal of the Air & Waste Management Association*, vol. 70, no. 2, pp. 228–242, 2020.

[13] J. Wahlström, L. Olander, and U. Olofsson, "Size, shape, and elemental composition of airborne wear particles from disc brake materials," *Tribology Letters*, vol. 38, pp. 15–24, 2010.

[14] B. D. Garg, S. H. Cadle, P. A. Mulawa, P. J. Groblicki, C. Laroo, and G. A. Parr, "Brake wear particulate matter emissions," *Environmental Science & Technology*, vol. 34, no. 21, pp. 4463–4469, 2000.

[15] P. G. Sanders, N. Xu, T. M. Dalka, and M. M. Maricq, "Airborne brake wear debris: size distributions, composition, and a comparison of dynamometer and vehicle tests," *Environmental science & technology*, vol. 37, no. 18, pp. 4060–4069, 2003.

[16] A. Iijima, K. Sato, K. Yano, M. Kato, K. Kozawa, and N. Furuta, "Emission factor for antimony in brake abrasion dusts as one of the major atmospheric antimony sources," *Environmental science & technology*, vol. 42, no. 8, pp. 2937–2942, 2008.

[17] L. Storch, C. Hamatschek, D. Hesse, F. Feist, T. Bachmann, P. Eichler, and T. Grigoratos, "Comprehensive analysis of current primary measures to mitigate brake wear particle emissions from light-duty vehicles," *Atmosphere*, vol. 14, no. 4, p. 712, 2023.

[18] K. Liew and U. Nirmal, "Frictional performance evaluation of newly designed brake pad materials," *Materials & Design*, vol. 48, pp. 25–33, 2013.

[19] A. Thorpe and R. M. Harrison, "Sources and properties of non-exhaust particulate matter from road traffic: a review," *Science of the total environment*, vol. 400, no. 1-3, pp. 270–282, 2008.

[20] Encyclopedia of the Environment, "Airborne particulate matter and their health effects." `https://www.encyclopedie-environnement.org/en/health/airborne-particulate-health-effects/`. Accessed online 2024-03-27.

[21] United Nations Economic Commission for Europe, "Report of the GRPE Particle Measurement Programme (PMP) Government Sponsored Work Programmes July 2003." `https://unece.org/DAM/trans/doc/2003/wp29grpe/TRANS-WP29-GRPE-specinf01e.pdf`. Accessed online 2024-04-08.

[22] Dekati, "ELPI+." `https://dekati.com/products/elpi/`. Accessed online 2024-04-08.

[23] A. Järvinen, M. Aitomaa, A. Rostedt, J. Keskinen, and J. Yli-Ojanperä, "Cali-

bration of the new electrical low pressure impactor (ELPI+)," *Journal of aerosol science*, vol. 69, pp. 150–159, 2014.

[24] Rocky Mountain Labs, "Difference between SEM and EDX analysis." https://rockymountainlabs.com/sem-and-edx-analysis/. Accessed online 2024-04-09.

[25] A. Mohammed and A. Abdullah, "Scanning electron microscopy (SEM): A review," in *Proceedings of the 2018 International Conference on Hydraulics and Pneumatics—HERVEX, Băile Govora, Romania*, vol. 2018, pp. 7–9, 2018.

[26] ThermoFisher Scientific, "Edx analysis with SEM: How Does it Work?." https://www.thermofisher.com/blog/materials/edx-analysis-with-sem-how-does-it-work/. Accessed online 2024-08-27.

[27] Biltema, "Drawing of the brake pad used for this thesis." https://www.biltema.se/en-se/car---mc/car-spare-parts/brake-system/brake-friction/brake-pads/brake-pads-2000038210. Accessed online 2024-08-24.

A

Appendix 1

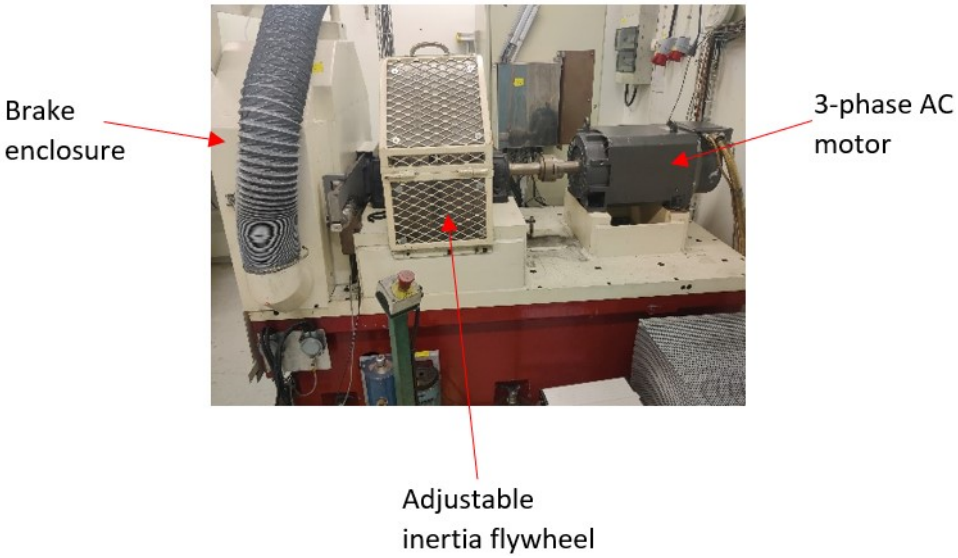

Figure A.1: Electric motor and the driveline

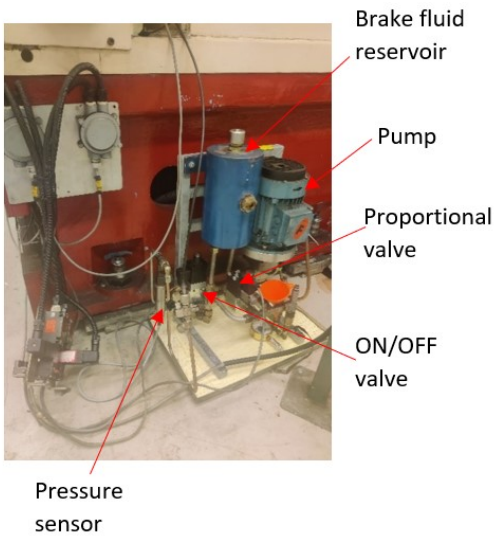

Figure A.2: Brake Unit with valves, brake fluid tank, pump and pressure sensor

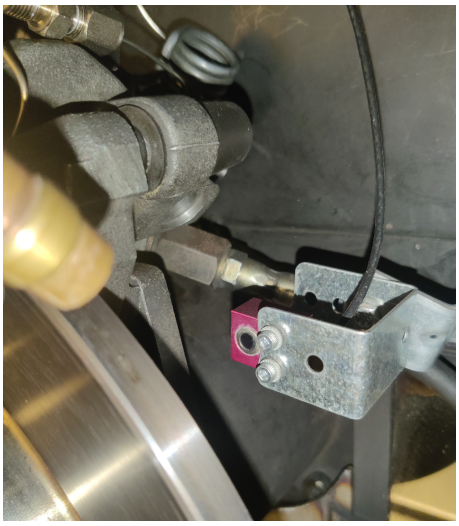

Figure A.3: Infra-red camera to capture disc temperature

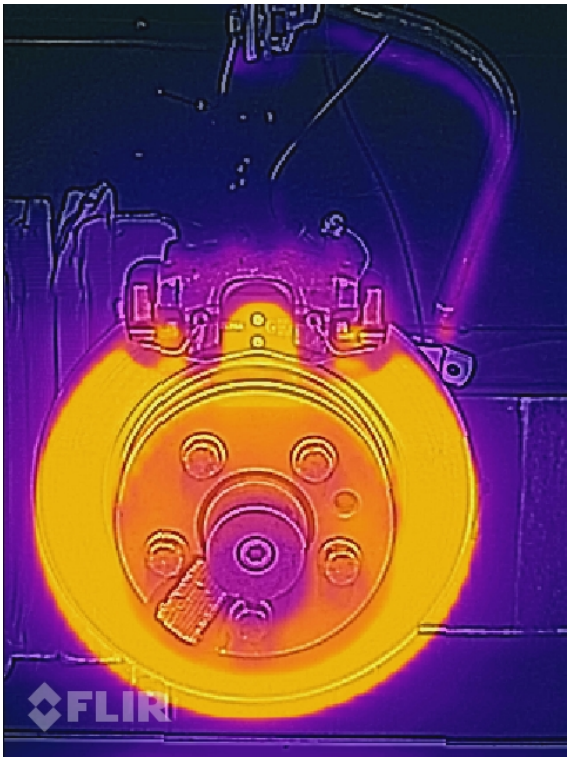

Figure A.4: Forward Looking Infrared (FLIR) image of hot brake disc at 150°C

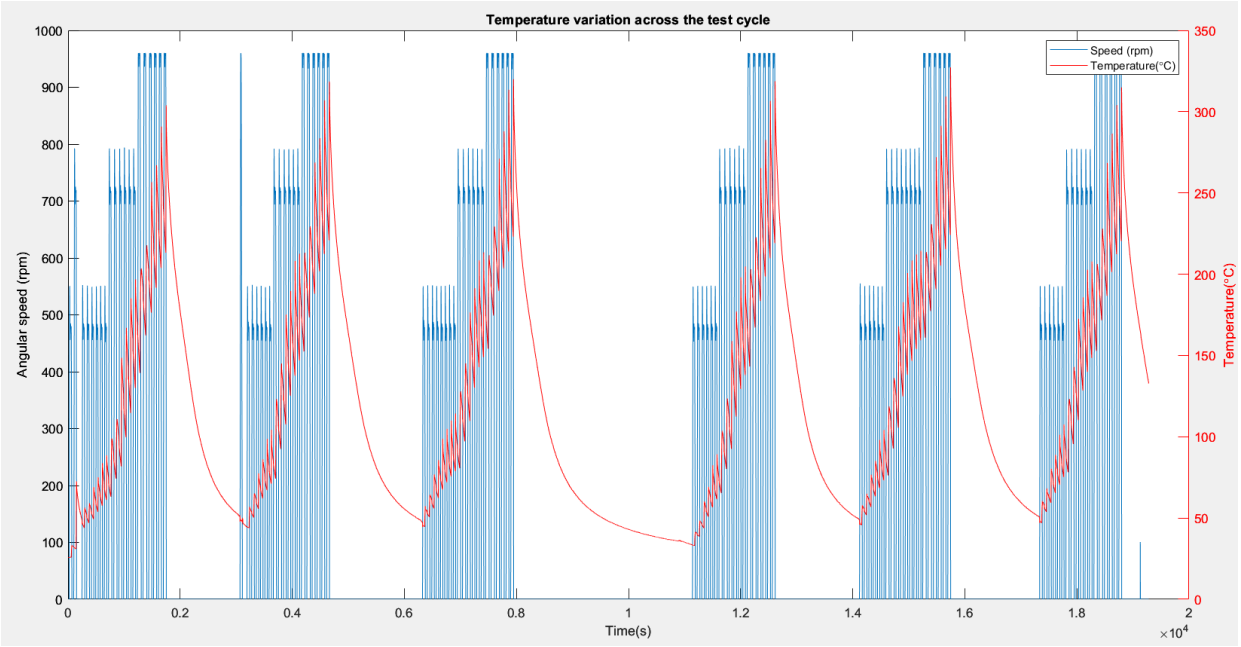

Figure A.5: Temperature of the brake disc measured by the IR camera

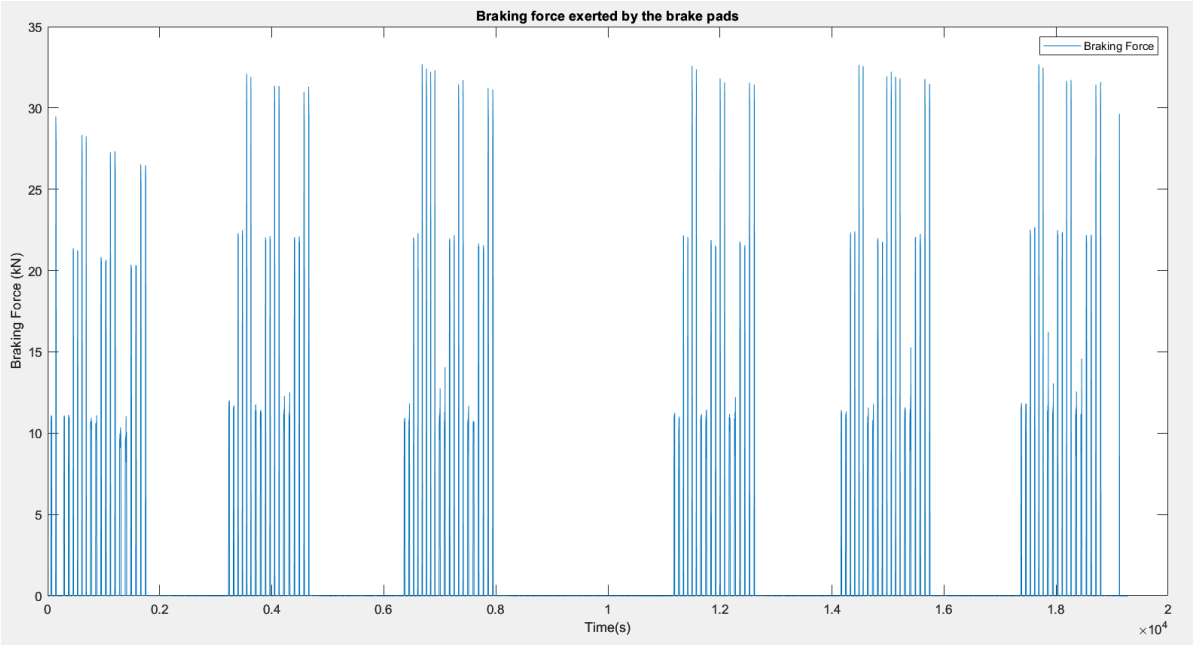

Figure A.6: Braking force

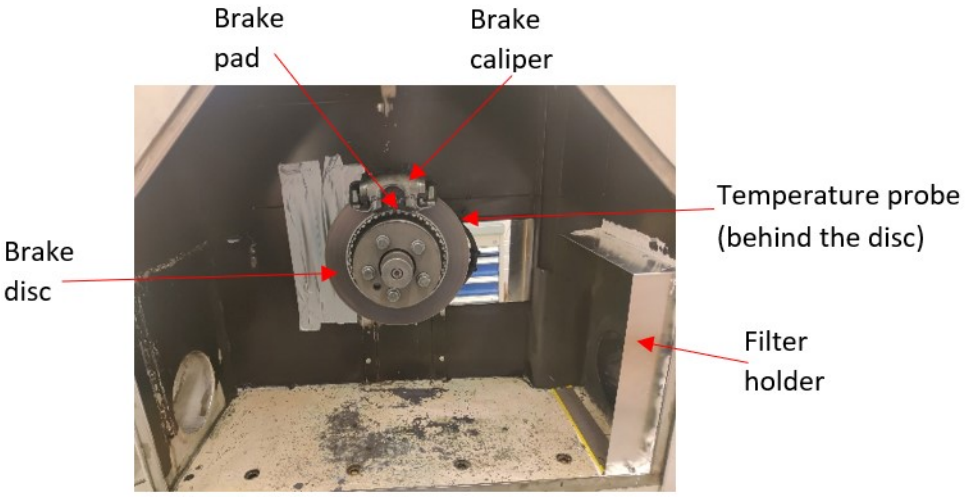

Figure A.7: Inside the brake enclosure

Elements	Stage No	C	O	Si	P	S	K	Ca	Mn	Fe	Cl	Cr	Ni	Th	Tb	Ag
Test4_22	5	55.14	24.28	8.43	0	0.49	0.85	0	1.27	7.19	2.34	0	0	0	0	0
Test4_23	5	34.73	35.57	0	0	2.46	0.59	1.83	0.36	24.46	0	0	0	0	0	0
Test4_24	5	34.44	20.83	3.61	0	1.5	0.48	0.63	1.23	29.89	0	4.1	3.3	0	0	0
Test4_25	5	62.55	20.03	5.86	0	0.43	0.71	0.52	1.04	8.87	0	0	0	0	0	0
Test4_26	5	28.8	35.47	9.68	0	1.3	1.12	1.28	0.96	20.87	0	0	0	0	0	0.51
Test4_27	5	29.47	26.55	4.26	0	0.41	0.53	2.93	0.61	35.22	0	0	0	0	0	0
Test4_28	5	22.28	34.28	4.84	0	0.53	0.32	2.5	0.45	34.8	0	0	0	0	0	0
Test4_29	5	37.05	30.54	4.74	0	1.66	3.42	1.39	0.73	20.01	0.46	0	0	0	0	0
Test4_30	5	23.4	18.51	0	0	0	0	0	3.43	54.65	0	0	0	0	0	0
Test4_31	5	53.38	25.19	6.87	0	0.38	0	0.52	1.86	11.8	0	0	0	0	0	0
Test4_32	5	26.46	31.78	4.84	0	1.74	0.3	2.09	0.73	32.06	0	0	0	0	0	0
Test4_33	5	25.48	32.95	9.6	0	1.23	0.18	2.29	0.85	27.43	0	0	0	0	0	0
Test4_34	5	22.53	37.92	8.41	0	0.82	0	2.16	0.59	27.59	0	0	0	0	0	0
Test4_35	5	34.01	30.95	10.85	0	1.14	0.28	1.8	0.6	20.36	0	0	0	0	0	0
Test5_36	7	24.18	27.73	3.52	0.28	1.32	0.19	3.3	0	39.47	0	0	0	0	0	0
Test5_37	7	23.01	23.63	3.75	0.14	1.82	0.17	4.04	0	43.45	0	0	0	0	0	0
Test5_38	7	19.9	23.16	0	0	1.7	0.2	3.32	0.73	50.99	0	0	0	0	0	0
Test5_39	7	60.61	24.16	0	0	1.27	0	0.94	0.83	12.19	0	0	0	0	0	0
Test5_40	7	25.91	30.74	2.76	0.14	1.87	0	2.62	0.61	34.9	0.45	0	0	0	0	0
Test5_41	7	26.54	33.08	3.43	0	0.99	0.16	2.83	0.5	32.47	0	0	0	0	0	0
Test5_42	7	30.65	30.01	2.77	0.39	2.63	0	2.61	0.65	30.28	0	0	0	0	0	0
Test5_43	7	28.54	28.54	2.76	0.42	2.69	0.2	2.8	0.71	33.33	0	0	0	0	0	0
Test5_44	7	18.22	30.79	0	0	0	0	3.59	0.86	46.54	0	0	0	0	0	0
Test5_45	7	28.99	37.95	0	0	0	0	1.97	2.24	28.85	0	0	0	0	0	0
Test6_46	9	26.02	30.87	0	0	0	0.12	3.65	0.5	38.84	0	0	0	0	0	0
Test6_47	9	24.3	28.03	0	0	0	0	2.46	2.77	36.97	0	0	0	5.47	0	0
Test6_48	9	28.74	26.75	0	0	0	0	4.04	0.54	39.93	0	0	0	0	0	0
Test6_49	9	23.51	23.73	1.44	0	0.07	0.16	4.63	0	46.45	0	0	0	0	0	0
Test6_50	9	22.02	24.38	1.43	0	0.05	0.14	5.1	0	46.88	0	0	0	0	0	0
Test7_51	10	23.37	23.82	0	0	0	0	3.45	2.24	47.11	0	0	0	0	0	0
Test7_52	10	21.28	21.28	1.33	0	0	0.14	4.89	0.53	50.56	0	0	0	0	0	0
Test7_53	10	23.53	27.02	0	0	0	0	4.22	0.53	44.69	0	0	0	0	0	0
Test7_54	10	21.15	29.21	1.46	0	0	0.16	4.17	0	43.83	0	0	0	0	0	0
Test7_55	10	24.6	25.97	1.41	0	0	0	4.24	0.35	42.35	0	0	0	0	1.08	0
Test8_56	12	15.74	12.82	0.92	0	0	0.09	3.01	0.53	66.88	0	0	0	0	0	0
Test8_57	12	25.82	21.25	0	0	0	0	4.42	0.91	47.6	0	0	0	0	0	0
Test8_58	12	19.75	19.65	1.25	0	0	0.12	4.68	0.52	54.02	0	0	0	0	0	0
Test8_59	12	22.75	27.64	0	0	0	0.17	4.59	0.78	44.07	0	0	0	0	0	0
Test8_60	12	26.93	24.38	0	0	0	0	2.71	3.46	42.52	0	0	0	0	0	0
Test8_61	12	19.18	20.87	1.07	0	0	0.14	6.2	0	52.55	0	0	0	0	0	0
Test8_62	12	24.53	30.38	0	0	0	0	2.95	1.88	40.26	0	0	0	0	0	0

Figure A.8: Weight% of all the detected elements

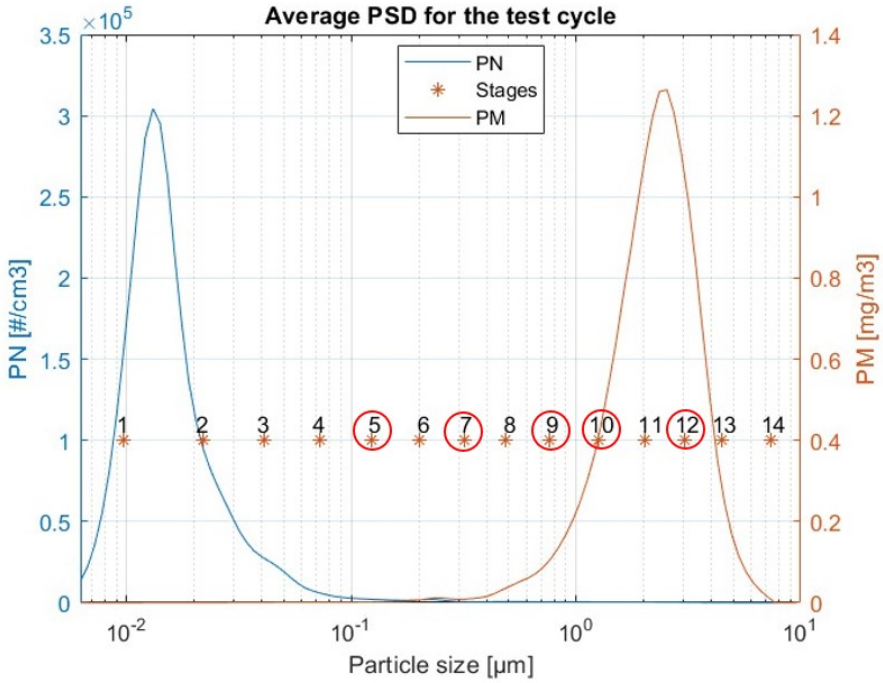

Figure A.9: Average PSD for the test cycle with the selected stages highlighted

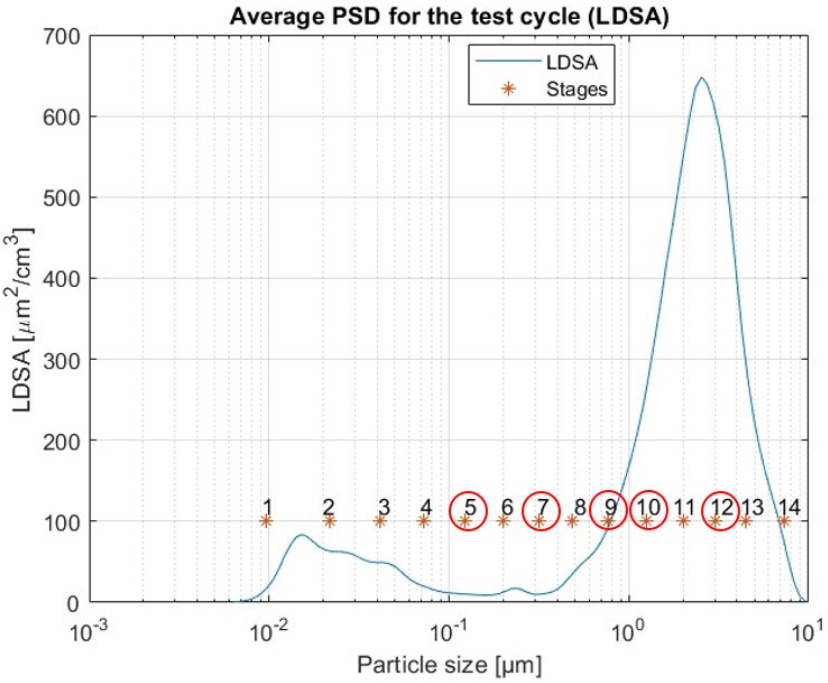

Figure A.10: Average LDSA plot for the test cycle with the selected stages highlighted

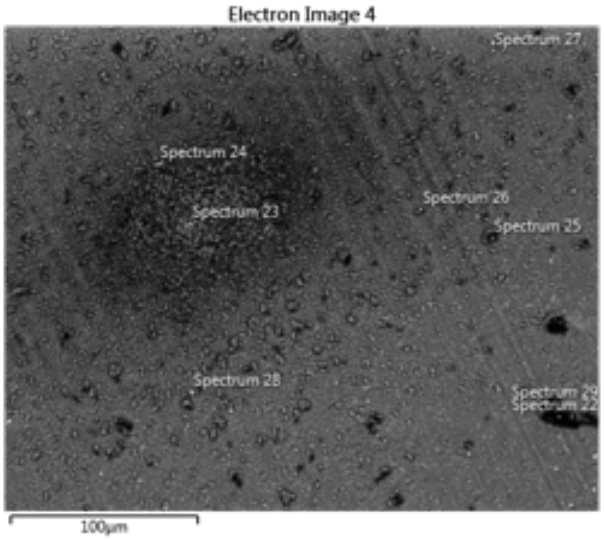

Figure A.11: Image acquired using microscope from Oxford instruments (Stage 5)

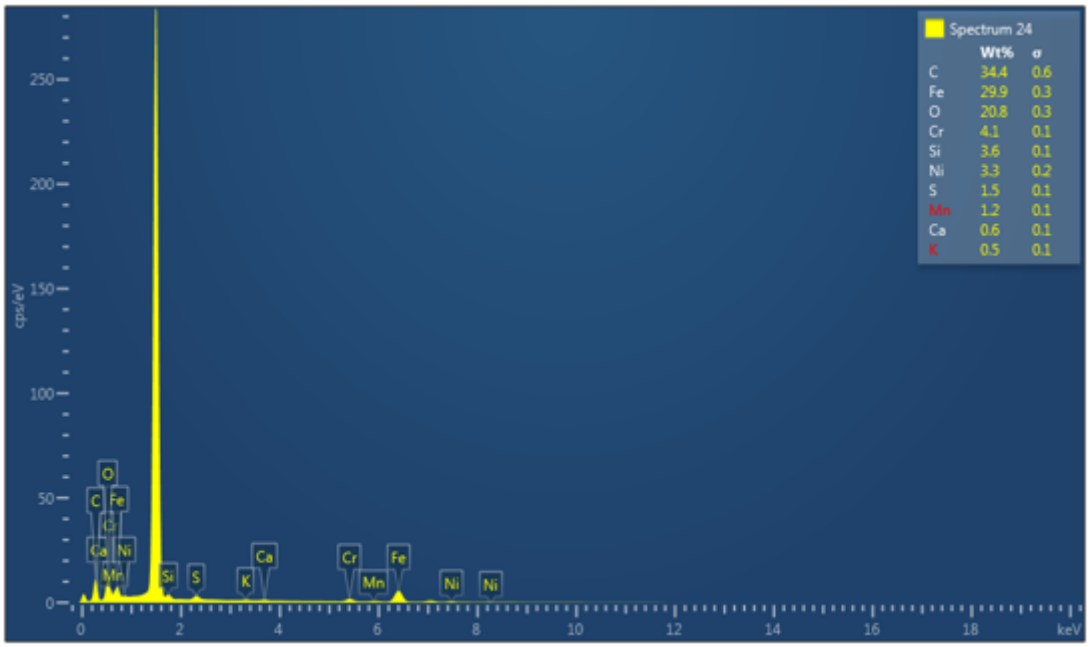

Figure A.12: An SEM result for Stage 5 using microscope from Oxford instruments

DEPARTMENT OF MECHANICS AND MARITIME SCIENCES
CHALMERS UNIVERSITY OF TECHNOLOGY
Gothenburg, Sweden 2024
www.chalmers.se

CHALMERS
UNIVERSITY OF TECHNOLOGY